The Steady-State Atmospheric Circulation Response to Climate Change–like Thermal Forcings in a Simple General Circulation Model

AMY H. BUTLER, DAVID W. J. THOMPSON, AND ROSS HEIKES

Department of Atmospheric Science, Colorado State University, Fort Collins, Colorado

(Manuscript received 28 April 2009, in final form 11 February 2010)

ABSTRACT

The steady-state extratropical atmospheric response to thermal forcing is investigated in a simple atmospheric general circulation model. The thermal forcings qualitatively mimic three key aspects of anthropogenic climate change: warming in the tropical troposphere, cooling in the polar stratosphere, and warming at the polar surface. The principal novel findings are the following:

1) Warming in the tropical troposphere drives two robust responses in the model extratropical circulation: poleward shifts in the extratropical tropospheric storm tracks and a weakened stratospheric Brewer–Dobson circulation. The former result suggests heating in the tropical troposphere plays a fundamental role in the poleward contraction of the storm tracks found in Intergovernmental Panel on Climate Change (IPCC)-class climate change simulations; the latter result is in the opposite sense of the trends in the Brewer–Dobson circulation found in most previous climate change experiments.

2) Cooling in the polar stratosphere also drives a poleward shift in the extratropical storm tracks. The tropospheric response is largely consistent with that found in previous studies, but it is shown to be very sensitive to the level and depth of the forcing. In the stratosphere, the Brewer–Dobson circulation weakens at midlatitudes, but it strengthens at high latitudes because of anomalously poleward heat fluxes on the flank of the polar vortex.

3) Warming at the polar surface drives an equatorward shift of the storm tracks. The storm-track response to polar warming is in the opposite sense of the response to tropical tropospheric heating; hence large warming over the Arctic may act to attenuate the response of the Northern Hemisphere storm track to tropical heating.

4) The signs of the tropospheric and stratospheric responses to all thermal forcings considered here are robust to seasonal changes in the basic state, but the amplitude and details of the responses exhibit noticeable differences between equinoctial and wintertime conditions. Additionally, the responses exhibit marked nonlinearity in the sense that the response to multiple thermal forcings applied simultaneously is quantitatively different from the sum of the responses to the same forcings applied independently. Thus the response of the model to a given thermal forcing is demonstrably dependent on the other thermal forcings applied to the model.

1. Introduction

There is increasing evidence that anthropogenic forcing has driven and will drive several robust changes in the extratropical circulation. Among the most robust changes are poleward shifts in the extratropical storm tracks consistent with positive trends in the northern and southern annular modes of variability. Observations reveal robust positive trends in the southern annular mode (SAM) during austral spring/summer that are consistent with forcing by the Antarctic ozone hole (Thompson and Solomon 2002). Observations also reveal positive trends in the northern annular mode (NAM; Hurrell 1995; Thompson et al. 2000), albeit the trends in the NAM have weakened since the late 1990s (e.g., Overland and Wang 2005).

Similar behavior is found in climate models. Numerical simulations forced by the observed stratospheric ozone depletion are capable of reproducing the amplitude, structure, and seasonality of the observed trend in the SAM (Gillett and Thompson 2003; Arblaster and Meehl 2006; Miller et al. 2006), and simulations forced by future ozone recovery reveal a SAM trend in the opposite sense (Son et al. 2008). Numerical simulations forced with increasing atmospheric carbon dioxide also reveal marked positive trends in the annular modes, with more robust trends in the Southern Hemisphere

Corresponding author address: Dr. Amy H. Butler, NOAA/NCEP/Climate Prediction Center, 5200 Auth Road, Camp Springs, MD 20746.
E-mail: amy.butler@noaa.gov

DOI: 10.1175/2010JCLI3228.1

(Shindell et al. 1999; Fyfe et al. 1999; Kushner et al. 2001; Cai et al. 2003; Shindell and Schmidt 2004; Brandefelt and Kallen 2004; Yin 2005; Miller et al. 2006; Arblaster and Meehl 2006; Lu et al. 2008). In fact, the tropospheric storm-track responses to future increases in greenhouse gases and past Antarctic ozone depletion are among the most robust circulation changes found in the Intergovernmental Panel on Climate Change (IPCC) Fourth Assessment Report (AR4) runs (Hegerl et al. 2007).

Why are trends in the annular modes so ubiquitous in both observations of past and simulations of future climate change? Presumably, the annular modes (and hence the latitude of the extratropical jet and storm track) are sensitive to spatial gradients in the temperature field induced by stratospheric ozone depletion and increasing greenhouse gases. Unfortunately, the extratropical storm-track response to spatially varying thermal forcing is difficult to assess in observations, and only a handful of studies have examined the response of the atmospheric circulation to thermal forcing in numerical models. Polvani and Kushner (2002) and Kushner and Polvani (2004) examined the response of a simple atmospheric general circulation model (AGCM) to polar stratospheric cooling. Gerber and Polvani (2009) and Chan and Plumb (2009) revealed the sensitivity of the results in Polvani and Kushner (2002) to the presence of topography and the tropospheric equilibrium temperature profile, respectively. Son and Lee (2005), Ring and Plumb (2008), and Lim and Simmonds (2008) documented the circulation response to thermal forcing at both tropical and high latitudes. Eichelberger and Hartmann (2005) explored the effects of heating in the tropical troposphere on the strength of the stratospheric Brewer–Dobson circulation. Haigh et al. (2005) and Simpson et al. (2009) examined the response to heating in the tropical stratosphere. Lorenz and DeWeaver (2007) considered the effect of anthropogenically induced changes in tropopause height on the extratropical circulation.

The above studies are groundbreaking in that they are among the first to examine the AGCM response to thermal forcing in an idealized context. But numerous aspects of the atmospheric circulation response to thermal forcing remain to be addressed, particularly with regard to the response to anthropogenic forcing. For example, the experiments in Polvani and Kushner (2002) are relevant for understanding the annular mode response to Antarctic ozone depletion, but the sensitivity of their results to changes in the altitude and shape of the polar stratospheric cooling is unknown. The tropical heating profile in Son and Lee (2005) is much narrower than the expected response to increasing greenhouse gases, and their analysis is focused largely on the effects of tropical and polar heating on the number of jets in the extratropical circulation. Eichelberger and Hartmann (2005) do not consider the response of the tropospheric flow to the imposed tropical tropospheric heating and do not test the sensitivity of their results to changes in the shape of the forcing. Lim and Simmonds (2008) focus only on the Southern Hemisphere storm track response to tropical tropospheric heating, do not consider the sensitivity of their response to changes in the location and scale of the forcing, and use a full physics AGCM rather than the idealized configuration used here. Haigh et al. (2005) and Simpson et al. (2009) focus on the thermal effects of the solar cycle in the tropical stratosphere. Lorenz and DeWeaver (2007) focus on the height of the tropopause—not the thermal forcing itself—as the key forcing mechanism.

The goal of this study is to identify and document the role of select thermal forcings in driving large-scale changes in the atmospheric circulation. We focus on the three principal heatings most commonly associated with anthropogenic forcing: enhanced warming in the tropical troposphere (which mimics increased latent heating by condensation of water vapor in the free tropical troposphere), enhanced cooling in the polar stratosphere (which mimics the cooling associated with polar ozone depletion), and enhanced warming at the surface over the polar regions (which mimics the heating associated with snow–ice–albedo feedback in the Arctic). The analyses are designed not to provide quantitatively precise reproductions of the full IPCC-class model response to anthropogenic forcing, but rather to identify the relative importance of different thermal forcings in driving the large-scale changes in the atmospheric circulation that are so pervasive in such simulations.

In section 2, we discuss the model and model climatology. In section 3, we present the results for thermal forcings centered in the tropical troposphere, polar stratosphere, and polar surface. In section 4, we review the sensitivity of the results to multiple forcings applied simultaneously and to changes in the background state. In the final section, we summarize the key findings and speculate on the role of different forcing mechanisms in driving the simulated responses. A quantitative assessment of the forcing mechanisms is forthcoming in a companion paper.

2. Model description and climatology

The experiments are run on the dry dynamical core of the Colorado State University general circulation model (CSU GCM; Ringler et al. 2000). The vertical coordinate is hybrid sigma/isentropic (Konor and Arakawa 1997), and the model is discretized in the horizontal using a geodesic grid (Heikes and Randall 1995). The vertical coordinate transitions smoothly from sigma ($\sigma = p/p_s$)

near the surface to isentropic in the free troposphere and stratosphere, and the geodesic grid is constructed from an icosahedron through recursive division of each triangular face. The advantages of the geodesic grid are that it has no singularity at the poles and has approximately homogeneous and isotropic resolution throughout the globe (Heikes and Randall 1995); the advantages of the hybrid vertical coordinate are that it benefits from terrain-following sigma coordinates near the earth's surface but quasi-Lagrangian isentropic coordinates aloft (Konor and Arakawa 1997).

The parameters used in the control run are identical to those specified in Held and Suarez (1994). All experiments are run with no topography, with 10 242 geodesic horizontal grid cells (which yields a resolution of ~250 km) and 25 vertical layers with the model top at 1 hPa. The experiments are integrated for 2160 days with a model time step of 80 s. The first 360 days of all runs are discarded to account for initial spinup, which leaves 1800 days for the analysis of each run (the zonal-mean wind and temperature fields both reach their long-term mean values within ~200 days).

All runs are considered using an equinoctial radiative equilibrium temperature profile specified in Held and Suarez (1994) with the exception of the experiments in section 4, which are adapted to wintertime conditions. The control climatology of the model run under equinoctial conditions is shown in Fig. 1. The top panel shows the climatological-mean, zonal-mean temperature, and eddy heat fluxes; the middle panel shows the climatological-mean, zonal-mean zonal wind, and eddy momentum fluxes. In both panels, the dark black lines indicate the approximate height of the tropopause, which is estimated as the pressure level where the lapse rate (dT/dz) changes sign. The eddy momentum and heat fluxes are found as $\overline{u'v'}$ and $\overline{v'T'}$, respectively, where the overbars denote the zonal-mean and the primes denote departures from the zonal-mean. The eddy fluxes are calculated on daily time scales before being averaged over all days in the integration.

Consistent with Held and Suarez (1994), the zonal-mean zonal wind is westerly throughout the upper troposphere poleward of ~10° latitude and peaks around 30 m s^{-1} near 250 hPa and 45° latitude. The largest eddy momentum fluxes are found near ~250 hPa between ~30° and 40° latitude, and hence the surface flow is westerly poleward of ~40° but easterly equatorward of ~30° latitude. The tropopause height is approximately 210 hPa at the poles and 110 hPa at the tropics (the tropopause height is highly variable across the axis of the model jet and is thus not shown in the subtropics).

The eddy heat fluxes exhibit two distinct maxima: one near the surface at ~40° latitude; the other near 200 hPa at ~45° latitude (Fig. 1a). The former lies along the largest gradient in surface temperature and is consistent with the generation of baroclinic waves in the lower troposphere; the latter reflects the flux of wave activity into the model stratosphere and thus the driving of the model Brewer–Dobson circulation. The model stratospheric residual circulation is evidenced by the reversal of the stratospheric equator-to-pole temperature gradient above ~250 hPa (Fig. 1a) and—as discussed in the following section—the poleward residual circulation at stratospheric levels. We will consider the effects of changing the model climatology to a wintertime radiative equilibrium temperature profile in section 4.

The leading pattern of variability in the model wind field is shown in Fig. 1c (note that the top panels are shown from pole to pole, but that the bottom panel is shown for only one hemisphere). Here the leading pattern of variability is defined as the first empirical orthogonal function (EOF) of the zonal-mean zonal wind field and is found by 1) removing the long-term mean from the zonal-mean wind field, 2) weighting the zonal-mean zonal wind field by the square root of the cosine of latitude and density, and 3) eigenanalyzing the covariance matrix for the region poleward of 20° latitude from 1000 hPa to the model top. The EOF and its associated momentum fluxes are found by regressing the zonal wind and momentum flux fields onto standardized values of the resulting leading principal component time series. The leading EOF of the zonal flow is reminiscent of those found in other simple AGCMs (e.g., Robinson 1991; Yu and Hartmann 1993; Ring and Plumb 2007; Gerber et al. 2008) and is characterized by out-of-phase fluctuations in the zonal-mean zonal wind field with centers of action located near 35° and 55° latitude and by anomalously poleward momentum fluxes near 250 hPa and 45° latitude. The pattern in Fig. 1c is hereafter referred to as the model annular mode, and its positive polarity is defined as periods when the momentum fluxes are anomalously poleward across 45° latitude.

The time scale of the model annular mode is important since the amplitude of its response to external forcing is directly related to the model decorrelation time scale (Ring and Plumb 2008; Gerber et al. 2008). As noted in Gerber et al. (2008) and Chan and Plumb (2009), experiments with very long model annular mode time scales (e.g., as in Kushner and Polvani 2004) are thought to have unrealistically large responses to external forcing. The time scale of the annular mode can be improved by increasing the spatial resolution of the model, adding zonal asymmetries such as topography, or adjusting model parameters such as the momentum and thermal damping (Gerber and Vallis 2007). The time scale can also be improved by increasing the amplitude

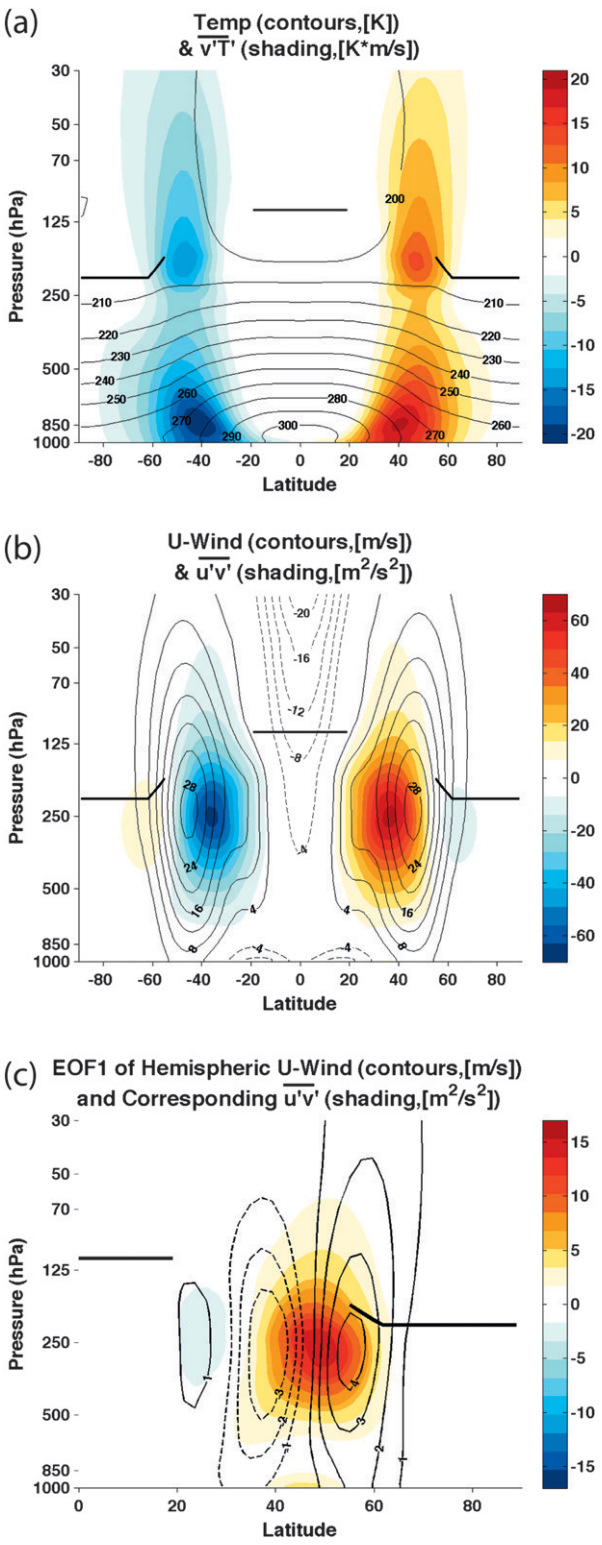

FIG. 1. The model control climatology for the equinoctial basic state. Bold black lines in all plots represent the control run tropopause height. (a) Contours: zonal-mean temperature (K). Shading: eddy heat flux (K m s^{-1}). (b) Contours: zonal-mean zonal wind (m s^{-1}). Shading: eddy momentum flux (m^2 s^{-2}). (c) Contours: leading EOF of the zonal-mean zonal wind poleward of 20° latitude. Units are m s^{-1} per standard deviation of the principal component (PC) time series. Shading: eddy momentum flux anomalies regressed onto the PC time series of the zonal-mean zonal wind (m^2 s^{-2} per standard deviation of the PC time series).

of the stratospheric wave drag and variability (e.g., Norton 2003). The decorrelation time scale of the annular mode in the model used here is ~26 days (±4.4 days as per the error estimate given in Gerber et al. 2008) for equinoctial conditions, which is comparable to the time scale of the observed annular modes (~10–20 days) and is close to the benchmark range proposed by Gerber et al. (2008). As mentioned in section 4, the time scale of the annular mode increases substantially under wintertime conditions (~176 days), in agreement with Chan and Plumb (2009) who note that the time scale is dependent on the tropospheric background state.

We quantify the component of the model response that projects onto the model annular mode (outlined in Table 5 below). The annular mode fit is found by 1) regressing the surface zonal wind response onto the surface component of the annular mode shown in Fig. 1c and 2) multiplying the full annular mode pattern in Fig. 1c by the resulting regression coefficient (e.g., Kushner et al. 2001).

3. The model response to climate change–like thermal forcings

In this section we document and explore the response of the CSU AGCM to three thermal forcings, which are designed to qualitatively mimic the primary spatially varying heatings associated with anthropogenic emissions of carbon dioxide and ozone-depleting substances. The forcings are 1) enhanced warming in the tropical troposphere, which mimics increased latent heating by condensation of water vapor at low latitudes; 2) enhanced cooling in the polar stratosphere, which mimics the cooling associated with polar ozone depletion; and 3) enhanced warming at the surface over the polar regions, which mimics the heating associated with the snow–ice–albedo feedback in the Arctic. The analytic functions for all thermal forcings are summarized in Table 1. In all results, the ''response'' to a given forcing is defined as the differences between the long-term means of the perturbed and control simulations. As noted in the introduction, the experiments are designed to explore the robustness and structure of the AGCM atmospheric circulation response to climate change–like thermal forcings, and not to provide quantitatively precise reproductions of the full IPCC-class response to

TABLE 1. Description of heating runs.

Heating run	Equation for forcing x = lat (radians), y = sigma level	$\sigma_x, \sigma_y, x_o, y_o$	Center of heating ± half depth (lat)	Center of heating ± half depth (pressure)
Heating in tropical upper troposphere (Fig. 2a)	$q_o \exp\left\{-\left[\frac{(x-x_o)^2}{2\sigma_x^2}+\frac{(y-y_o)^2}{2\sigma_y^2}\right]\right\}$	$\sigma_x = 0.4, x_o = 0$ $\sigma_y = 0.11, y_o = 0.3$	0° ± 27°	300 ± 125 mb
Shallow heating in tropical upper troposphere (Fig. 2b)	Same as Fig. 2a	$\sigma_x = 0.4, x_o = 0$ $\sigma_y = 0.07, y_o = 0.3$	0° ± 27°	300 ± 75 mb
Narrow heating in tropical upper troposphere (Fig. 2c)	Same as Fig. 2a	$\sigma_x = 0.21, x_o = 0$ $\sigma_y = 0.11, y_o = 0.3$	0° ± 13.5°	300 ± 125 mb
Heating in tropical middle troposphere (Fig. 2d)	Same as Fig. 2a	$\sigma_x = 0.4, x_o = 0$ $\sigma_y = 0.11, y_o = 0.5$	0° ± 27°	500 ± 125 mb
Cooling in lower polar stratosphere (Fig. 5a)	$q_o \exp\left\{-2\left[\frac{(x-x_o)^2}{2\sigma_x^2}+\frac{(y-y_o)^2}{2\sigma_y^2}\right]\right\}$	$\sigma_x = 0.4, x_o = 1.57$ $\sigma_y = 0.14, y_o = 0.1$	90°–18°	100 ± 115 mb
Cooling in midpolar stratosphere (Fig. 5b)	Same as Fig. 5a	$\sigma_x = 0.4, x_o = 1.57$ $\sigma_y = 0.10, y_o = 0.075$	90°–18°	75 ± 80 mb
Cooling in upper polar stratosphere (Fig. 5c)	Same as Fig. 5a	$\sigma_x = 0.31, x_o = 1.57$ $\sigma_y = 0.03, y_o = 0.05$	90°–13.5°	50 ± 25 mb
Shallow cooling in lower stratosphere (Fig. 6a)	$q_o \exp\left\{-\left[\frac{(x-x_o)^2}{2\sigma_x^2}+\frac{(-7000\ \ln y+7000\ \ln y_o)^2}{2\sigma_y^2}\right]\right\}$	$\sigma_x = 0.28, x_o = 1.57$ $\sigma_y = 2100, y_o = 0.2$	90°–18°	200 mb ± 2.5 km
Figure 6b	Same as Fig. 6a	$\sigma_x = 0.28, x_o = 1.57$ $\sigma_y = 2100, y_o = 0.175$	90°–18°	175 mb ± 2.5 km
Figure 6c	Same as Fig. 6a	$\sigma_x = 0.28, x_o = 1.57$ $\sigma_y = 2100, y_o = 0.15$	90°–18°	150 mb ± 2.5 km
Heating at polar surface (Fig. 7)	for $x > 0, q_o[\cos(x-x_o)]^{15} e^{6(y-y_o)}$ for $x < 0, 0$	$x_o = 1.57, y_o = 1$	90°–16°	1000–125 mb
Combination of Figs. 2a, 5a, and 7 (Fig. 8)	Sum of Figs. 2a, 5a, and 7			

TABLE 2. Zonal-mean temperature response at 100 mb averaged 60°–90° for the tropical tropospheric heating runs in Fig. 2. NS = not significant (<90% significance).

Heating run	Mean temperature response 100 mb, 60°–90° [difference (K), significance]
Heating in tropical upper troposphere (Fig. 2a)	−4.85, >99%
Shallow heating in tropical upper troposphere (Fig. 2b)	−2.61, >99%
Narrow heating in tropical upper troposphere (Fig. 2c)	−3.05, >99%
Heating in tropical middle troposphere (Fig. 2d)	−0.27, NS

TABLE 3. Zonal-mean temperature response at 100 mb averaged 0°–30° for the stratospheric cooling runs in Figs. 5 and 6. NS = not significant (<90% significance).

Heating run	Mean temperature response 100 mb, 0°–30° [difference (K), significance]
Cooling in lower polar stratosphere (Fig. 5a)	−0.17, NS
Cooling in midpolar stratosphere (Fig. 5b)	−0.04, NS
Cooling in upper polar stratosphere (Fig. 5c)	0.04, NS
Shallow cooling in lower stratosphere @ 200 mb (Fig. 6a)	0.20, NS
Shallow cooling in lower stratosphere @ 175 mb (Fig. 6b)	−0.49, >95%
Shallow cooling in lower stratosphere @ 150 mb (Fig. 6c)	0.04, NS

anthropogenic emissions. For this reason, the thermal forcings all have the same maximum amplitude (0.5 K day^{-1}); as such, variations in the response are due solely to changes in the structure and location of the forcing.

The significance of key features in the responses is documented in Tables 2–4 using a two-tailed test of the t statistic for the difference of means: Table 2 documents the significance of the polar stratospheric cooling in Fig. 2; Table 3 documents the significance of the tropical stratospheric temperature changes (as shown in Figs. 5 and 6); Table 4 documents the significance of the changes in the surface winds, eddy heat fluxes, and eddy momentum fluxes found in all figures. The number of independent samples (and thus the degrees of freedom) is assessed using the criteria outlined in Bretherton et al. (1999).

a. Heating in the tropical troposphere

In the first set of experiments, we examine the model response to zonally symmetric heating in the tropical troposphere. We consider first the forcing and responses shown in Fig. 2a. The left panel shows the thermal forcing, the middle panel shows the responses in the zonal-mean temperature field and the eddy heat flux, and the right panel shows the responses in the zonal-mean wind field and the eddy momentum flux. The forcing is centered at 300 hPa and the equator, and amplitudes greater than 0.25 K day^{-1} are limited to the region bounded by 175 hPa, 425 hPa, and 27° latitude (Table 1). There is weak heating (less than 0.1 K day^{-1}) in the lower tropical stratosphere, but, as demonstrated in the sensitivity experiments below, this feature has little bearing on the response. Since the forcing is symmetric about the equator, we show the response in only one hemisphere.

The response to the thermal forcing includes several pronounced features. In the temperature and eddy heat flux fields, these include (Fig. 2a, middle) 1) warming in the tropical troposphere that extends to ~45° latitude, 2) warming in the tropical stratosphere juxtaposed against cooling in the polar stratosphere, 3) increased poleward heat fluxes north of 50° juxtaposed against reduced poleward heat fluxes south of 50° latitude at most levels, and 4) a maximum in anomalous poleward heat fluxes in the upper troposphere near ~50° latitude and 300 hPa. In the wind and the eddy momentum flux fields, the most pronounced features include (Fig. 2a, right) 1) westerly anomalies that amplify with height between about 30°–70° latitude above 250 hPa, 2) anomalous westerly surface winds centered near 55° and anomalous easterly surface winds centered near 35° latitude, and 3) anomalous poleward momentum fluxes centered near 200 hPa and 45° latitude.

The warming of the tropical troposphere and the increase of the extratropical westerly wind shear above ~300 hPa are expected on the basis of the zonal-mean balanced response to the heating. But the other aspects of the response are not readily predicted by linear theory. In the troposphere, the pronounced changes in the eddy fluxes of heat and momentum are consistent with a poleward shift in the model storm track (the long-term mean eddy fluxes from the control and perturbed runs are superposed in Figs. 3a,b). The poleward contraction of the midlatitude storm tracks is accompanied by a poleward extension and weakening of the model Hadley cell circulation in the tropics (as indicated by the Eulerian-mean meridional streamfunction in Fig. 3c), a phenomenon also noted in observations and numerical simulations (Fu et al. 2006; Seidel and Randel 2007; Frierson et al. 2007; Lu et al. 2007, 2008; Seidel et al. 2008). Consistent with previous analyses of the AGCM response to thermal forcings (e.g., Polvani and Kushner 2002; Kushner and Polvani 2004) and the IPCC-model response to anthropogenic forcing (e.g., Miller et al.

TABLE 4. Zonal-mean eddy momentum flux ($m^2\ s^{-2}$), zonal wind U ($m\ s^{-1}$), and eddy heat flux ($K\ m\ s^{-1}$) response for the heating runs specified in the left column at levels and latitude bands indicated. NS = not significant (<90% significance).

Heating run	Eddy momentum flux response 250 mb, 45°–55° [difference ($m^2\ s^{-2}$), significance]	Surface U response, 55°–65° [difference ($m\ s^{-1}$), significance]	Eddy heat flux response, 100 mb, 0°–90° [difference ($K\ m\ s^{-1}$), significance]
Heating in tropical upper troposphere (Fig. 2a)	33.2, >99%	4.98, >99%	−0.87, >99%
Shallow heating in tropical upper troposphere (Fig. 2b)	26.7, >99%	3.96, >99%	−0.65, >99%
Narrow heating in tropical upper troposphere (Fig. 2c)	17.2, >99%	2.39, >99%	−0.49, >99%
Heating in tropical middle troposphere (Fig. 2d)	16.3, >99%	1.76, >99%	−0.22, >95%
Cooling in lower polar stratosphere (Fig. 5a)	12.8, >99%	2.67, >99%	0.43, >99%
Cooling in midpolar stratosphere (Fig. 5b)	7.71, >99%	1.68, >99%	0.35, >99%
Cooling in upper polar stratosphere (Fig. 5c)	−5.55, >99%	−0.83, >99%	0.02, NS
Shallow cooling in lower stratosphere (Fig. 6a)	10.0, >99%	1.28, >99%	−0.03, NS
Shallow cooling in lower stratosphere (Fig. 6b)	−10.5, >99%	−1.25, >99%	0.32, >99%
Shallow cooling in lower stratosphere (Fig. 6c)	−0.38, NS	0.02, NS	−0.01, NS
Heating at polar surface (Fig. 7)	−13.7, >99%	−1.83, >99%	−0.01, NS
Combination (Fig. 8b)	NH: 27.1, >99%	NH: 3.96, >99%	NH: −0.78, >99%
	SH: −41.8, >99%	SH: 6.90, >99%	SH: −0.64, >99%

2006), the eddy component of the tropospheric response to the heating in Fig. 2a projects strongly onto the positive polarity of the model annular mode; 97% of the hemispherically integrated root-mean-square changes in the surface wind are linearly congruent with the model annular mode (Table 5). Interestingly, in the subtropics the warming exhibits minima at stratospheric levels but maxima at tropospheric levels (Fig. 3d) that are reminiscent of similar features found in the observed temperature trends at those levels (Fu et al. 2006).

In the stratosphere, the out-of-phase temperature anomalies between polar and tropical latitudes are accompanied by a meridional dipole in the flux of wave activity into the stratosphere, with anomalously negative heat fluxes equatorward of 40° juxtaposed against anomalously positive heat fluxes poleward of 45° latitude (Fig. 2a, middle). The reduction in wave fluxes in subtropical latitudes is larger than the increase at polar latitudes, and thus the hemispheric-mean anomaly in stratospheric wave driving is negative (Table 4). The reduction in subtropical wave fluxes is associated with a weakening of the poleward residual circulation in the lowermost stratosphere (Fig. 4, dashed line; the meridional component of the residual circulation is calculated following the formulation in Andrews et al. 1987, section 3.5). The polar stratospheric cooling is statistically significant (Table 2), and both the meridional dipole in stratospheric temperatures and the diminished meridional residual flow are indicative of a weakening of the model Brewer–Dobson circulation.

The results in Fig. 2a thus reveal three key aspects of the AGCM response to tropical tropospheric heating:

1) a poleward contraction in the model storm tracks (and hence a shift toward the positive polarity of the model annular modes);
2) a weakening of the model Brewer–Dobson circulation;
3) a poleward expansion of the model Hadley cell circulation.

Recent studies have argued that the poleward shifts in the storm tracks found in the IPCC AR4 runs may be driven by tropical heating (e.g., Chen and Held 2007; Lu et al. 2007, 2008; Chen et al. 2008), and at least one study has revealed that the latitude of the SH storm track is sensitive to such heating in an AGCM (Lim and Simmonds 2008). The results in Fig. 2a confirm a direct linkage between tropical heating and the latitude of the storm tracks in the dry dynamical core of an AGCM. The inferred weakening of the model stratospheric overturning circulation is in the opposite sense of that found in experiments run on both simple (Eichelberger and Hartmann 2005) and complex (e.g., Rind 1998; Butchart and Scaife 2001; Li et al. 2008) climate models.

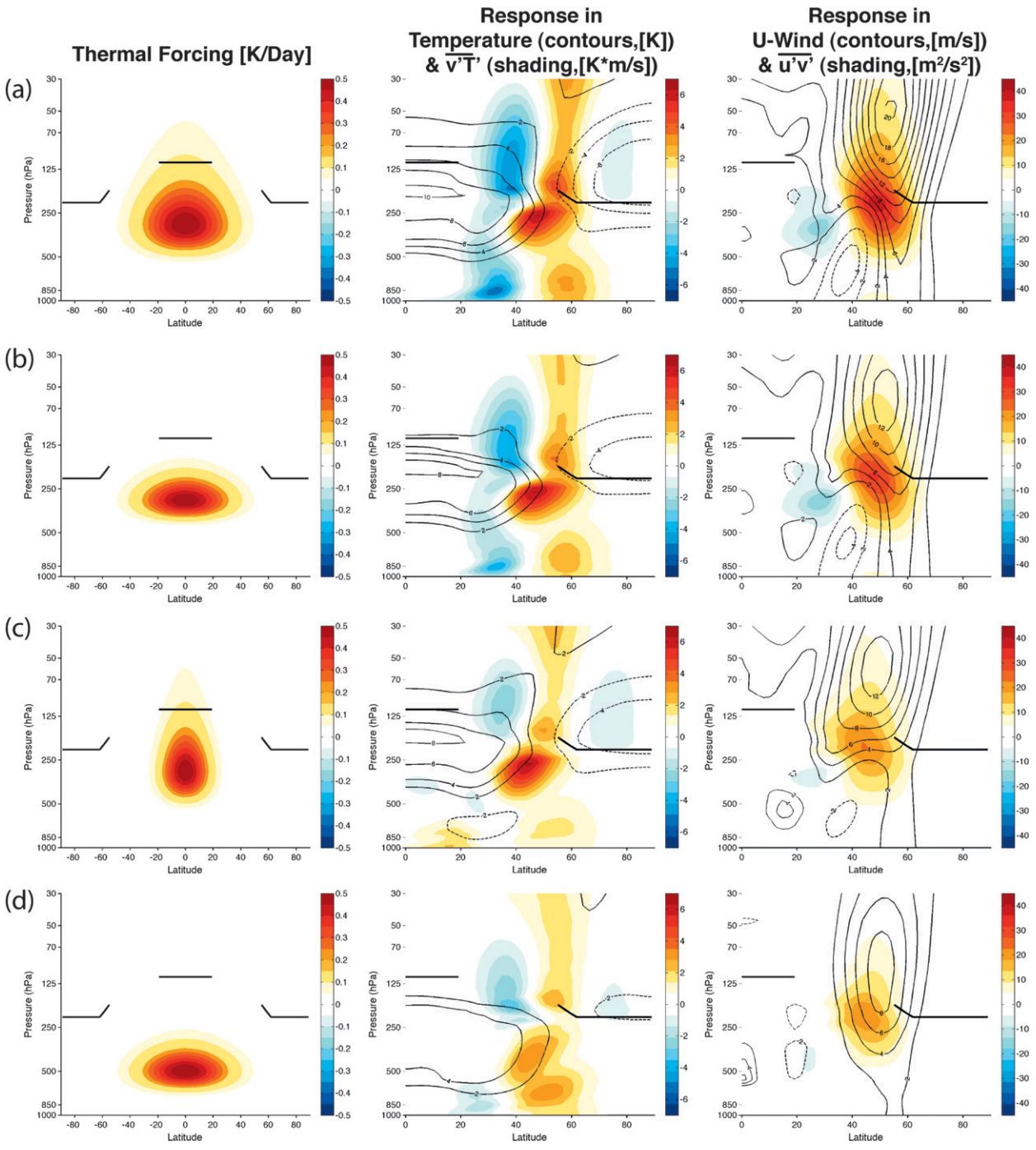

FIG. 2. The zonal-mean response to tropical tropospheric heating. Bold black lines in all plots represent the control run tropopause height. (left) The thermal forcing (K day^{-1}). (middle) The total eddy heat flux response (shading) (K m s^{-1}) and the temperature response (contours) (K). (right) The total eddy momentum flux response (shading) (m^2 s^{-2}) and the zonal-mean zonal wind response (contours) (m s^{-1}). (a) Results for tropical upper-tropospheric heating; (b) results for shallow tropical upper-tropospheric heating; (c) results for narrow tropical upper-tropospheric heating; (d) results for tropical heating centered at 500 hPa. Note the forcings are shown pole–pole but the responses are shown for only one hemisphere. The thermal forcings are detailed in Table 1.

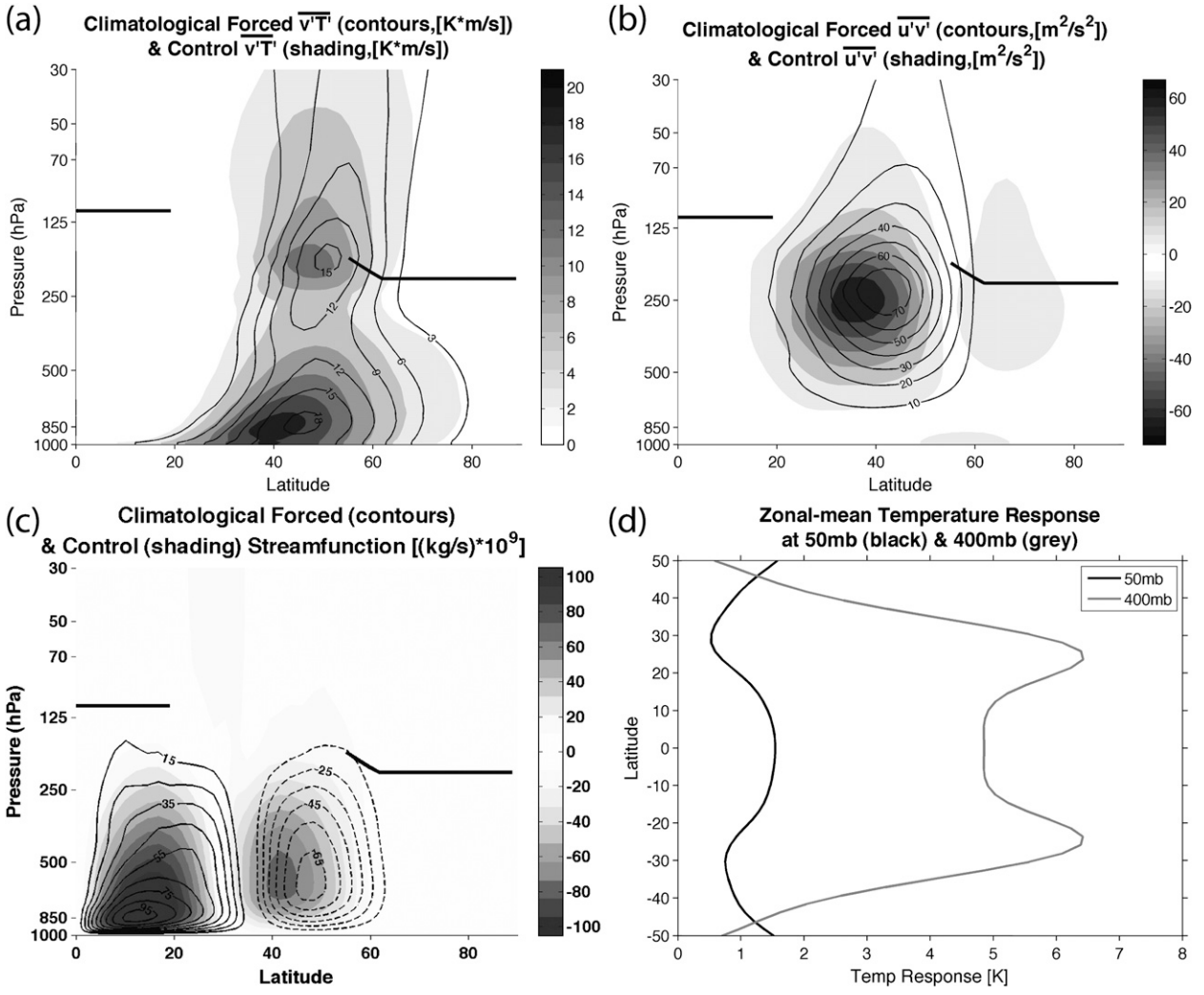

FIG. 3. Additional results from the forcing considered in Fig. 2a. (a) Long-term means of the total eddy heat fluxes from the forced (contours) and control (shading) runs (K m s^{-1}). Both contour intervals are 3 K m s^{-1}. (b) Long-term means of the total eddy momentum fluxes from the forced (contours) and control (shading) runs (m^2 s^{-2}). Both contour intervals are 10 m^2 s^{-2}. (c) Long-term means of the Eulerian-mean meridional streamfunction from the forced (contours) and control (shading) runs [(kg s^{-1}) × 10^9]. Solid contours correspond to clockwise circulation; dashed contours correspond to counterclockwise circulation. (d) The responses in zonal-mean temperatures from Fig. 2a highlighted at 50 mb (black) and 400 mb (gray) (K).

How robust are the key responses found in Fig. 2a? In Figs. 2b–d we examine the sensitivity of the model response to changes in the shape and altitude of the tropical heating. The results in Figs. 2b–d are derived from forcings similar to that used in Fig. 2a, except that in Fig. 2b the forcing is compressed vertically, in Fig. 2c it is compressed meridionally, and in Fig. 2d it is compressed vertically and lowered so that it is centered at 500 hPa. The analytic expressions for all thermal forcings are summarized in Table 1.

Compressing the heating in the vertical direction (Fig. 2b) weakens slightly the extratropical wind and temperature responses but overall has no effect on the key features of the response. The model jet and eddy fluxes are still shifted poleward, the model annular mode is still nudged toward its positive polarity, and the model Brewer–Dobson circulation is still weakened. Compressing the heating in the meridional direction (Fig. 2c) only slightly weakens the amplitude of the stratospheric response and has a more pronounced effect on the amplitude of the extratropical tropospheric response. But even in this case the tropospheric wind and eddy momentum fluxes are still shifted poleward, the eddy heat fluxes still exhibit a distinct maximum in the upper troposphere at ~40° latitude, and the surface eddy heat fluxes are still anomalously poleward at ~55° latitude. Interestingly, the meridional scale of the tropical tropospheric warming is unchanged between Figs. 2a and 2c,

TABLE 5. The rms of the surface wind responses averaged 0°–90°; the rms of the components of the response averaged 0°–90° that are linearly congruent with the model annular mode; and the corresponding percentage found by dividing the second column by the first.

Heating run	Rms of surface zonal wind (m s^{-1})	Rms of surface annular mode component (m s^{-1})	Percentage
Heating in tropical upper troposphere (Fig. 2a)	2.53	2.45	97%
Cooling in lower polar stratosphere (Fig. 5a)	1.29	1.10	85%
Heating at polar surface (Fig. 7)	0.98	0.91	93%

despite the fact that the imposed heating has been compressed substantially in the meridional direction. When the heating is compressed vertically and limited to the middle troposphere (Fig. 2d), the sign of the responses in the wind and temperature fields remain unchanged, but the amplitudes of the responses are diminished considerably, particularly in the polar stratosphere.

b. Cooling in the polar stratosphere

In the second set of experiments, we apply a zonally symmetric thermal forcing in the polar stratosphere, that is, in the region most strongly affected by Antarctic ozone depletion. We first consider the forcing shown in Fig. 5a. Here the cooling is centered at 100 hPa and damps to 0.25 K day^{-1} by 215 hPa and 72° latitude (Table 1). The cooling is analogous but not identical to that used in Polvani and Kushner (2002) and Kushner and Polvani (2004).

As expected from the zonal-mean balanced response, the thermal forcing is associated with cooling in the polar stratosphere (Fig. 5a, middle) and anomalous westerly shear in the extratropical stratosphere (Fig. 5a, right). But, as is the case for tropical heating, the response to polar stratospheric cooling also includes pronounced changes in the eddy fluxes of heat and momentum. The changes in the eddy fluxes are for the most part consistent with those found in Polvani and Kushner (2002). Cooling in the polar stratosphere drives increased poleward momentum fluxes across ~50° latitude and thus equivalent barotropic westerlies that extend from the surface to the lower stratosphere. As is the case for tropical heating, the changes in the zonal flow reflect a poleward shift in the model extratropical jet, and the barotropic component of the response projects strongly onto the positive polarity in the model annular mode (Table 5).

As is the case for tropical heating, the response to polar stratospheric cooling is marked by a meridional dipole in the flux of wave activity into the stratosphere (Fig. 5a, middle). But in this case the anomalously negative heat fluxes equatorward of 40° are considerably weaker than the anomalously positive heat fluxes poleward of 45° latitude at the tropopause level. The changes in the residual circulation (Fig. 4; gray line) reveal a weakening of the equator-to-pole residual flow equatorward of ~50° latitude but a strengthening of the residual flow at high latitudes. The anomalous downgradient stratospheric heat fluxes along the flank of the stratospheric vortex are consistent with enhanced wave driving in the polar stratosphere and are highly significant (Table 4, column 3).

Hence, the extratropical stratospheric response to polar stratospheric cooling (Fig. 5a) differs considerably from the response to tropical tropospheric heating (Fig. 2a), despite the fact both responses are associated with temperature falls in the polar stratosphere. In the case of tropical tropospheric heating (Fig. 2a), the polar temperature falls are driven adiabatically by changes in the stratospheric circulation, and the meridional residual flow is weakened at all latitudes. In the case of polar stratospheric cooling (Fig. 5a), the polar temperature falls are diabatically driven, and the meridional residual flow is weakened in the subtropics but strengthened at high latitudes (Fig. 4).

How sensitive to the location of the forcing is the circulation response to polar stratospheric cooling? In Figs. 5b,c we examine the effect of lifting the lower bound of

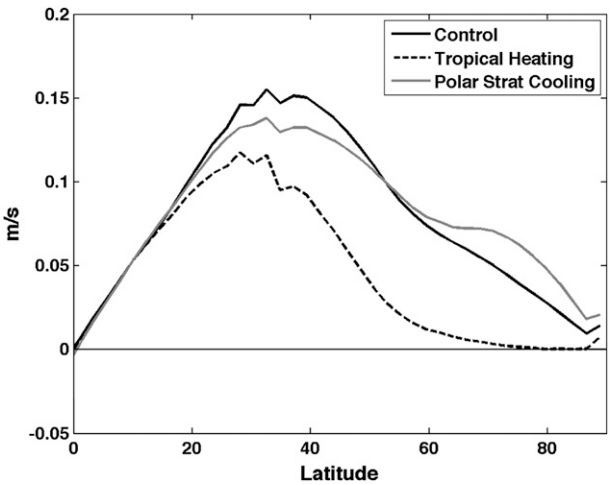

FIG. 4. Time-mean, zonal-mean residual meridional circulation (v^*) (m s^{-1}) for the equinoctial state runs: control (black line; Fig. 1), tropical tropospheric heating (dashed line; Fig. 2a), and polar stratospheric cooling (gray line; Fig. 5a). The residual circulation is calculated using the formulation outlined in Andrews et al. (1987, section 3.5).

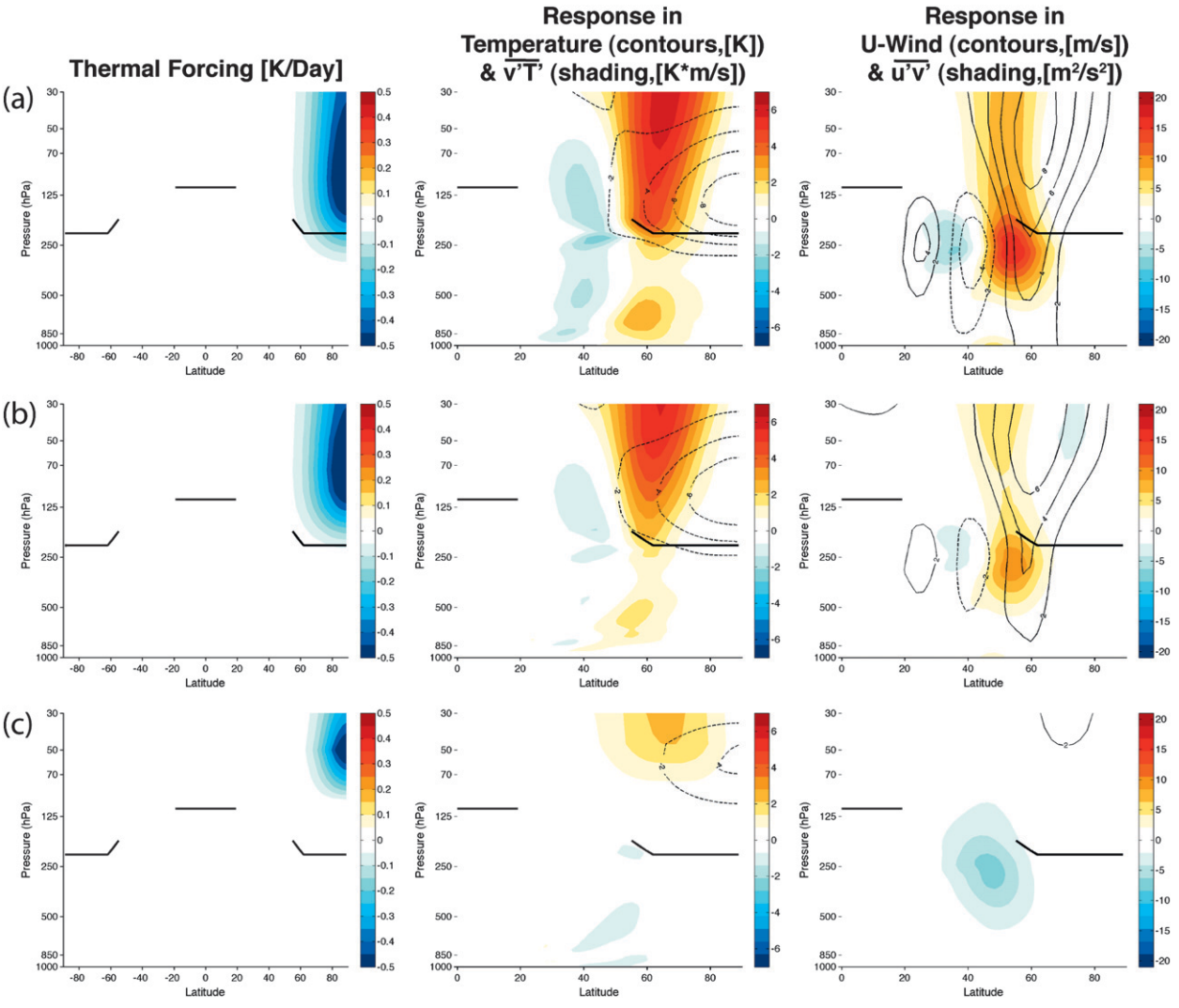

FIG. 5. As in Fig. 2, but for (left) the responses to the polar stratospheric thermal forcings. The forcings are documented in Table 1 and are centered at (a) 100, (b) 75, and 50 hPa (c). (right) Note the shading scaling is about half that for Fig. 2.

the cooling while continuing to allow the upper bound of the cooling to extend through the top of the stratosphere. When the center of the heating is lifted by 25 hPa (Fig. 5b), the amplitude of the response is damped by ~50%, but the structure of the response is unchanged and the key features remain significant: the heat fluxes are still anomalously positive in the polar stratosphere, the upper-tropospheric momentum fluxes are still anomalously poleward across 50° latitude, and the surface zonal flow is still anomalously easterly along ~40° and westerly along ~60° latitude (see also Table 4). However, when the center of the heating is lifted by 50 hPa (Fig. 5c), the barotropic component of the tropospheric response largely vanishes.

The sensitivity of the tropospheric response to polar stratospheric cooling is investigated further in Fig. 6. We again examine the effect of lifting the cooling, but in this case the depth of the cooling is only ~100 hPa. Figure 6a shows results for shallow cooling centered at 200 hPa. The structure of the response is largely unchanged from that shown in the top of Fig. 5, albeit the amplitude of the response is weaker. Note that in the case of shallow cooling the increased heat fluxes in the polar stratosphere are confined to the levels where cooling is occurring (Fig. 6a, middle panel). Figures 6b,c show results for the same shallow cooling, but in these cases the cooling has been lifted by 25 hPa (Fig. 6b) and 50 hPa (Fig. 6c). Lifting the cooling has little effect on the changes in polar stratospheric temperatures (middle column), but it has a dramatic effect on the changes in the tropospheric circulation (right column). When the cooling is lifted by 25 to 175 hPa (Fig. 6b), the tropospheric response

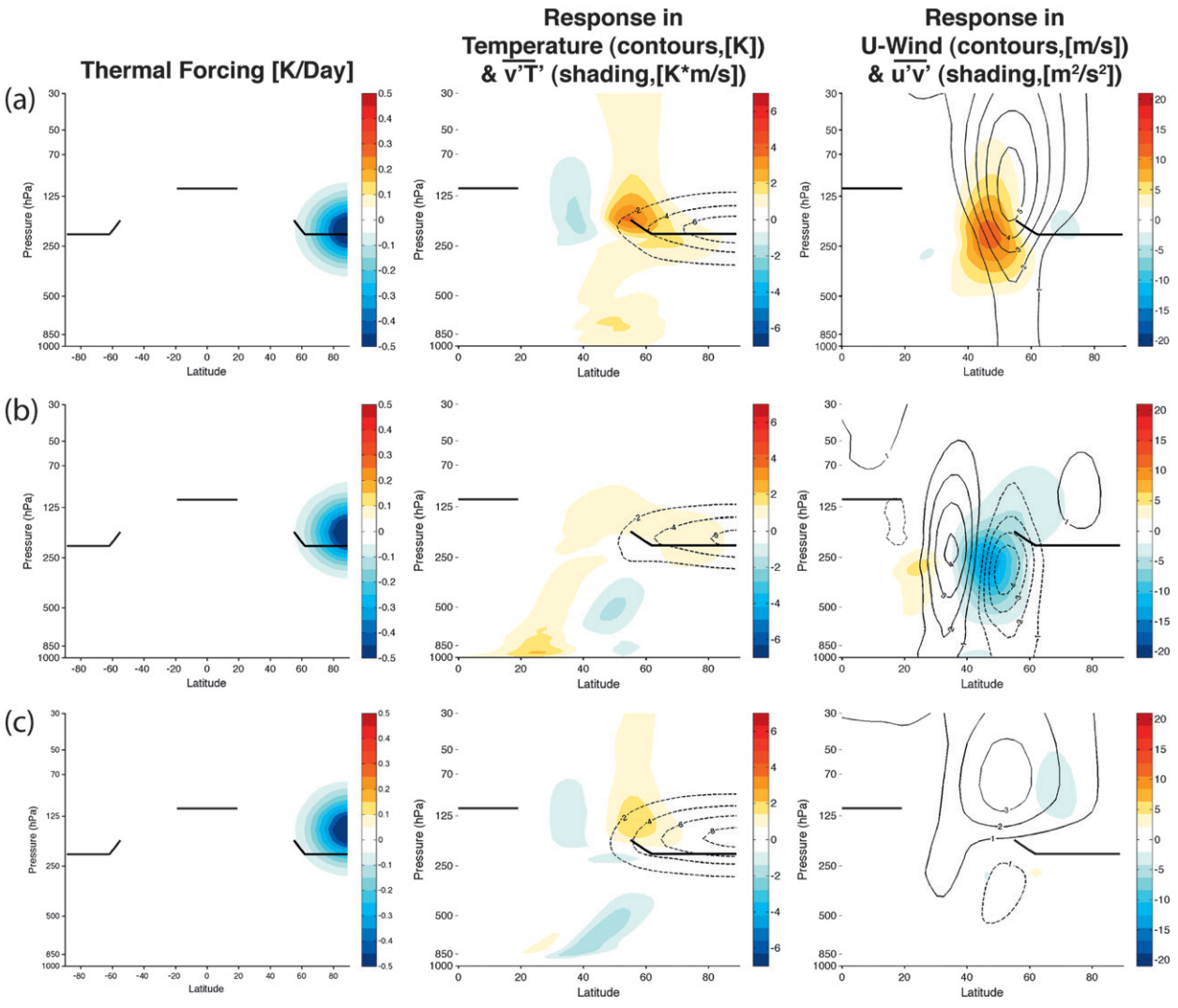

FIG. 6. As in Fig. 2, but for (left) the responses to the polar stratospheric thermal forcings. The forcings are documented in Table 1 and are centered at (a) 200, (b) 175, and (c) 150 hPa.

changes sign: the momentum fluxes are anomalously equatorward and the model jet is shifted equatorward (the equatorward momentum fluxes are statistically significant; Table 4). When the cooling is lifted by 50 to 150 hPa (Fig. 6c), the tropospheric response is negligible. Note that in all cases the vertical shear of the zonal flow is westerly in the upper troposphere along 60° latitude (as required by thermal wind): in Figs. 6a,c the shear is associated with increasing westerly anomalies with height; in Fig. 6b it is associated with weakening easterly anomalies with height.

c. Warming at the polar surface

The third forcing we examine is zonally symmetric heating at the surface over the pole, that is, the region predicted to warm most dramatically over the next century because of the snow–ice–albedo feedback over the Arctic. The heating is detailed in Table 1, and the structure of the heating and the corresponding responses are shown in Fig. 7. The tropospheric response is dominated by anomalously equatorward momentum fluxes across ~40° latitude, anomalously weak eddy heat fluxes at ~50° latitude, and significant barotropic wind anomalies at ~55° latitude and ~35° latitude. The changes in the momentum fluxes and zonal flow are statistically significant (Table 4) and project strongly onto the negative polarity of the model annular mode (Table 5). Hence the AGCM response to shallow polar warming is consistent with an equatorward shift in the model jet and is reminiscent of the midwinter response of the annular mode to predicted sea ice trends in fully coupled AGCMs (Deser et al. 2010). The annular mode response

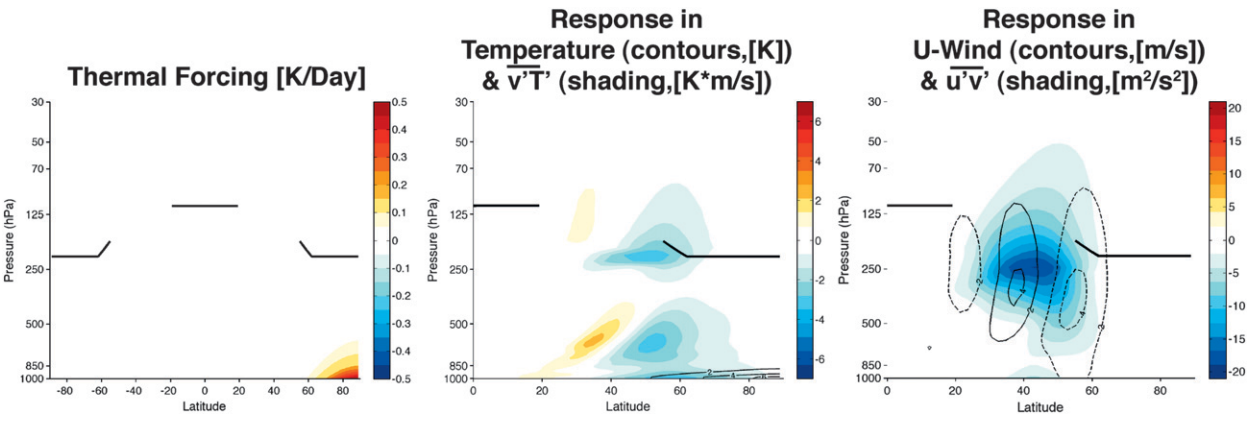

FIG. 7. As in Fig. 2, but for (left) the responses to the polar surface thermal forcing.

to polar warming is in the opposite sense of the response to both tropical tropospheric warming and polar stratospheric cooling.

4. Sensitivity to multiple thermal forcings and changes in the basic state

The atmospheric basic state likely plays an important role in determining the response of the eddy fluxes of heat and momentum to thermal forcing (e.g., Sigmond and Scinocca 2010). In this section, we examine the effects of the background state in two ways: 1) we examine the effects of applying multiple thermal forcings simultaneously, and 2) we examine the effects of changing the basic state from equinoctial to wintertime conditions.

a. Multiple thermal forcings

In Fig. 8 we examine the combined response to multiple forcings and then compare the results with the sum of the responses to the individual forcings. We consider three principal thermal forcings: the tropical tropospheric heating from Fig. 2a, the polar stratospheric cooling from Fig. 5a, and the polar surface warming from Fig. 7. The stratospheric cooling is limited to the SH to represent hemispheric asymmetries in ozone depletion; the polar surface warming is limited to the NH to represent hemispheric asymmetries in polar climate change. The combined forcing is shown in the top panel in Fig. 8; the responses to the combined forcing are shown in Fig. 8b; and the sums of the individual responses to the three forcings from Fig. 2a, Fig. 5a (applied to the SH), and Fig. 7 (applied to the NH) are shown in Fig. 8c.

The results in Fig. 8 confirm that the effects on the extratropical storm tracks of tropical tropospheric and polar surface warming are in the opposite sense. Thus the simulated response of the storm track to tropical tropospheric warming is mitigated in the Northern Hemisphere by Arctic warming, and this mitigation may provide an explanation for the relatively weak annular mode trends found in the NH in several climate change simulations (e.g., Miller et al. 2006). More surprisingly, the results in Fig. 8 highlight a high degree of nonlinearity in the response to multiple thermal forcings. The response to the combined forcings (Fig. 8b) is structurally similar but very different in amplitude to the sum of the individual responses (Fig. 8c), particularly in the SH. The most pronounced differences between the combined responses and the sum of the individual responses are stronger cooling in the SH and tropical stratosphere in the combined response (cf. the left panels in Figs. 8b,c) but larger tropospheric zonal wind anomalies in the summed responses (cf. the right panels in Figs. 8b,c). The results in Figs. 8b,c thus reveal that the amplitude of the response to a given thermal forcing is strongly dependent on the other thermal forcings applied to the system.

b. Changing the basic state from equinoctial to wintertime conditions

In Figs. 9–11 we examine the effects of changing the basic state from equinoctial to wintertime conditions on some of our key results. In the experiments described in section 3, the basic state is driven by relaxation to radiative equilibrium temperatures that approximate equinoctial conditions. The equinoctial basic state is associated with strong westerly jets that peak near 250 hPa and 45° latitude and decrease with height into the stratosphere (Fig. 1b). The extratropical stratospheric zonal flow is weakly westerly and thus permits the vertical propagation of Rossby waves. The stratospheric residual circulation is poleward throughout the stratosphere (Fig. 4; black line).

Figure 9 shows the model basic state for radiative equilibrium temperatures that approximate wintertime conditions. Here we use the wintertime equilibrium

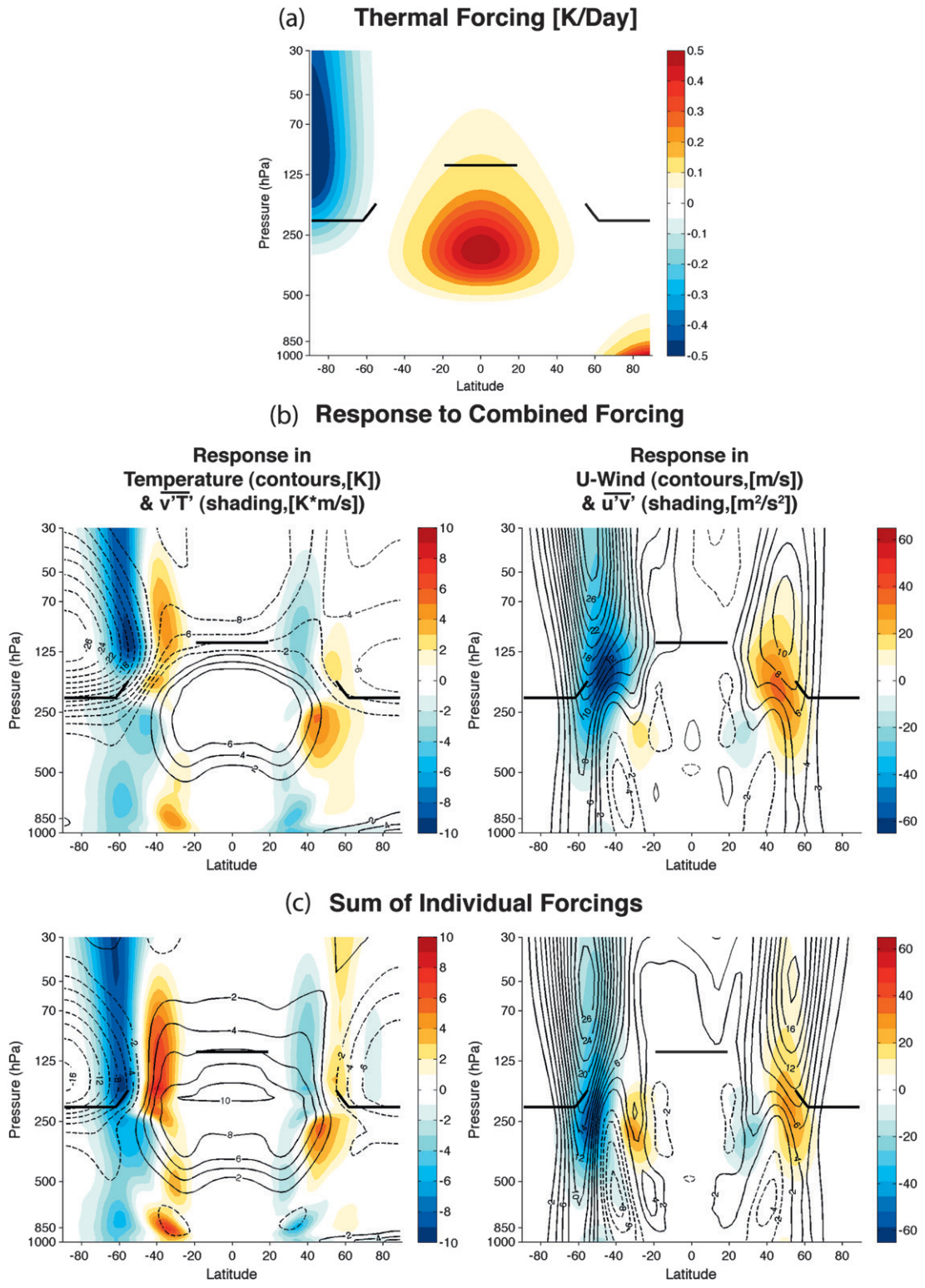

FIG. 8. (a) The combined forcing. (b) The responses to the combined forcing (results are organized as in the middle and right panels of Fig. 2). (c) The linear sum of the responses from Figs. 2a, 5a, and 7, where the responses in Fig. 5a are applied only to the Southern Hemisphere and the responses in Fig. 7 are applied only to the Northern Hemisphere. See text for details. Note that the shading scale is different than that in Fig. 2a.

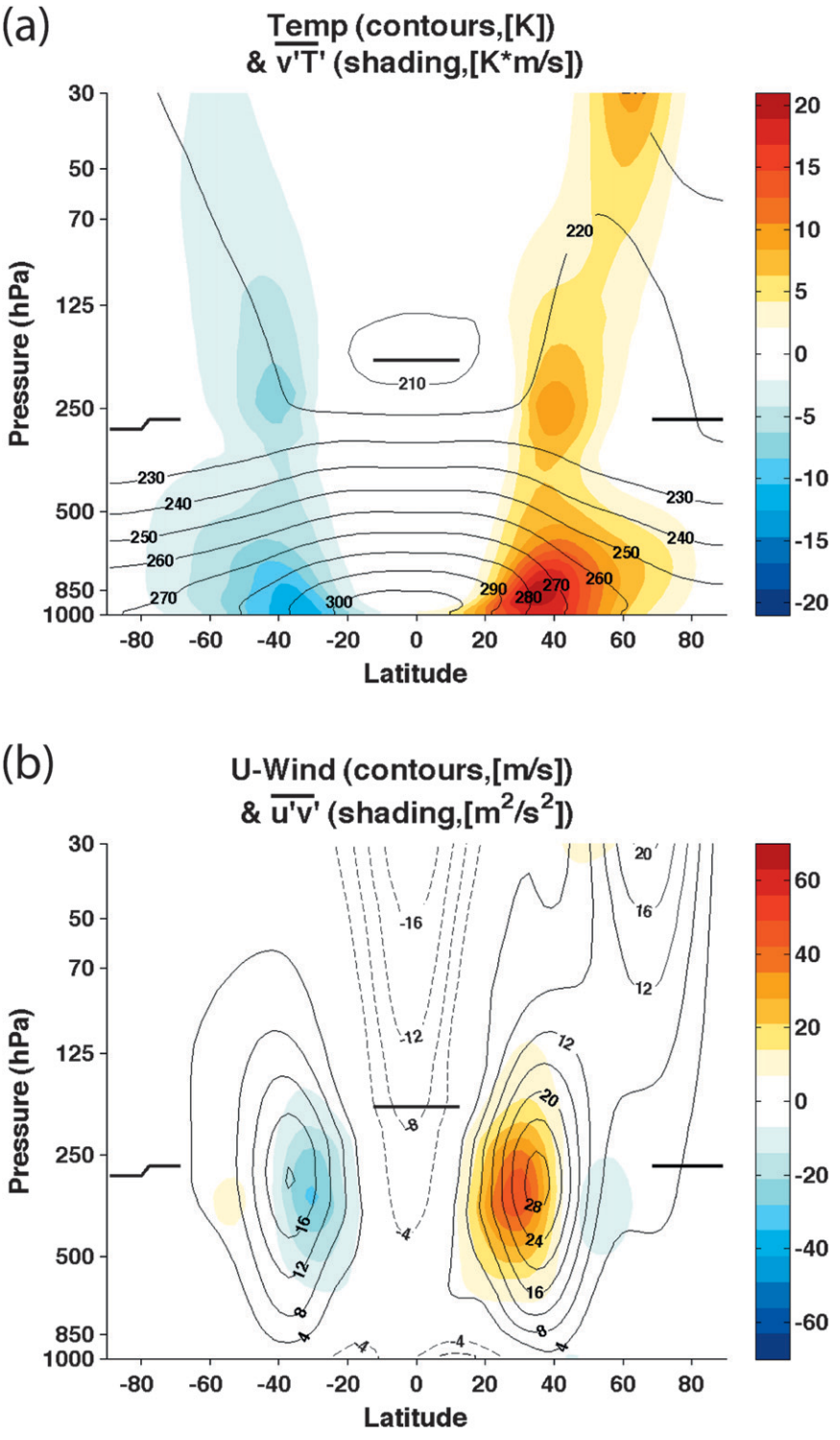

FIG. 9. As in Figs. 1a,b, but for the model control climatology for the wintertime basic state. Bold black lines in all plots represent the control run tropopause height. (a) Contours: zonal-mean temperature (K). Shading: eddy heat flux (K m s^{-1}). (b) Contours: zonal-mean zonal wind (m s^{-1}). Shading: eddy momentum flux (m^2 s^{-2}).

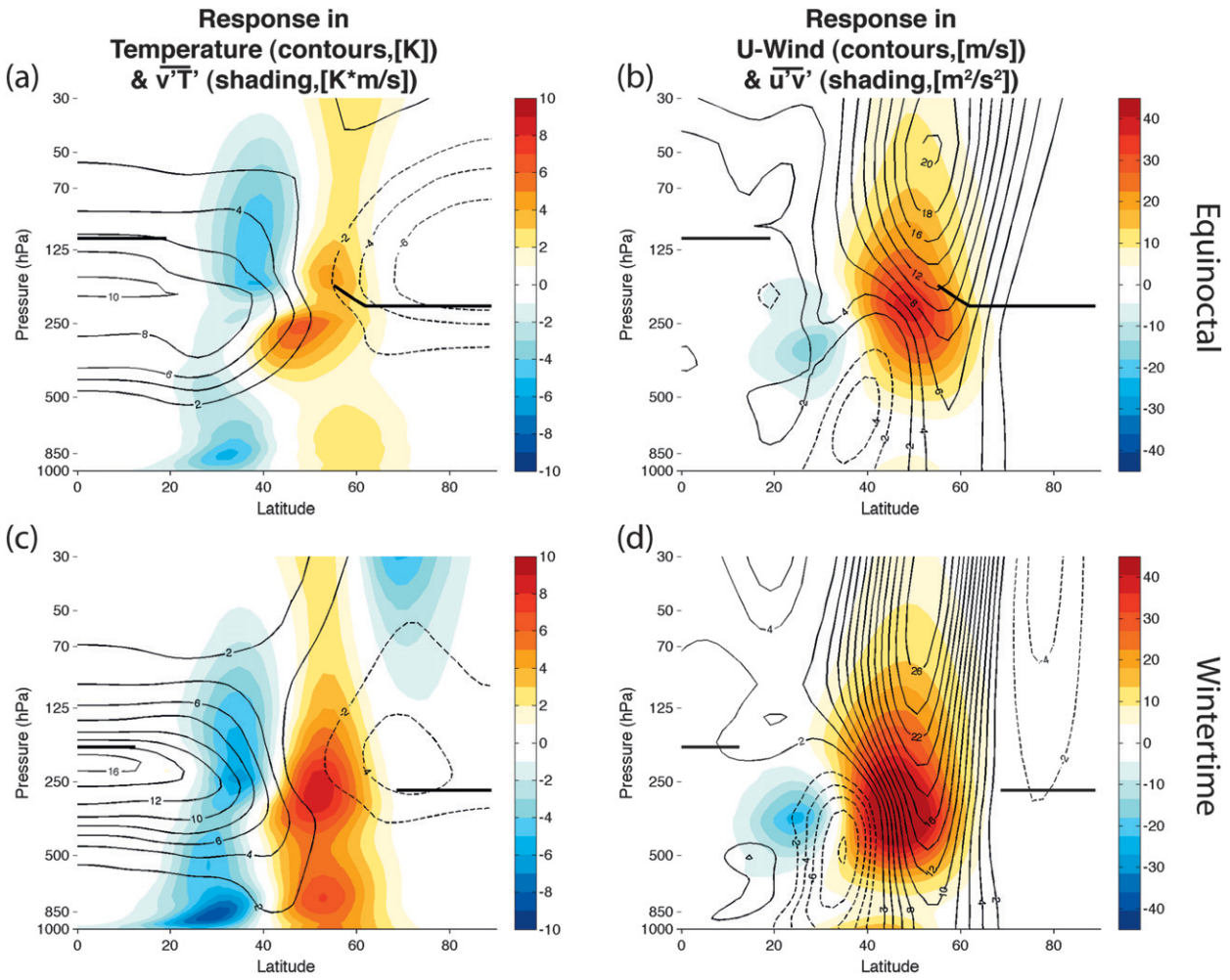

FIG. 10. The responses to the heating shown in the top left panel of Fig. 2a applied to different seasonal configurations of the flow. (top) The response when the heating is applied to the equinoctial basic state (results are reproduced from the middle and right panels in Fig. 2a). (bottom) The response to the same heating applied to the wintertime basic state. (left) The total eddy heat flux response (shading) (K m s^{-1}) and the temperature response (contours) (K). (right) The total eddy momentum flux response (shading) (m^2 s^{-2}) and the zonal-mean zonal wind response (contours) (m s^{-1}). Note that the shading scheme in the top panels is slightly different than that used in Fig. 2a to facilitate comparison with the wintertime runs.

temperature profile applied by Polvani and Kushner (2002; the basic state is defined as their $\gamma = 2$ configuration). The most pronounced differences in the model climate between the equinoctial and wintertime radiative conditions are found in the stratosphere: whereas the equinoctial basic state is associated with weak westerly flow and eddy heat fluxes that decrease with height through the lower midlatitude stratosphere (Fig. 1), the wintertime basic state includes a distinct polar stratospheric vortex (Fig. 9b) and a secondary maximum in heat fluxes in the middle stratosphere (Fig. 9a). As noted below, the stratospheric residual flow is more pronounced under equinoctial conditions than it is under wintertime conditions, which may reflect the filtering of small-scale Rossby waves by the stronger wintertime stratospheric flow (note that the model has no topography and thus weak planetary waves). The wintertime conditions given by Polvani and Kushner (2002) yield a somewhat lower tropical tropopause (~175 hPa) than the equinoctial conditions used in the previous section (~110 hPa).

Figure 10 examines the model response to the tropical tropospheric heating used in Fig. 2a, but applied to the wintertime basic state. The results in the top panel of Fig. 10 are a reproduction (from Fig. 2a) of the model response to the tropical heating applied to the equinoctial basic state; the results in the bottom panel of Fig. 10 show the model response to the same heating applied

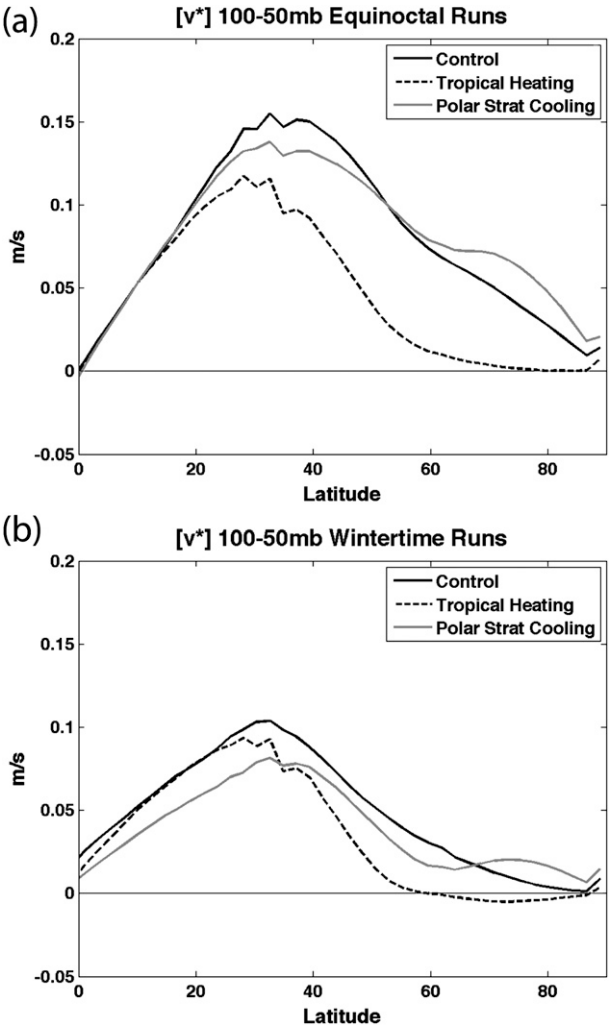

FIG. 11. Time-mean, zonal-mean residual meridional circulation (v^*) (m s^{-1}) for (a) the equinoctial basic-state runs (reproduction of Fig. 4) and (b) the wintertime basic-state runs. In both panels, the control results are indicated by black lines, the response to tropical tropospheric heating by the dashed lines, and the response to polar stratospheric cooling by the gray lines.

to the wintertime basic state. Similarly, Fig. 11a reproduces results from Fig. 4 for the model stratospheric residual circulation response under equinoctial conditions; Fig. 11b shows the model stratospheric response under wintertime conditions.

The key tropospheric responses to tropical heating are robust to seasonal changes in the basic state. The tropospheric heat and momentum fluxes are anomalously equatorward ~25°–30° latitude and anomalously poleward ~50° latitude, regardless of whether the model is run under equinoctial or wintertime conditions (Fig. 10). The key features of the tropospheric response are shifted equatorward by ~5° latitude and are considerably stronger under wintertime conditions. The stronger tropospheric circulation responses for the wintertime conditions are consistent with and may be related to the longer decorrelation time scales under this basic state (Chan and Plumb 2009).

The sign of the stratospheric responses to tropical heating are also robust to changes in the seasonal configuration. The residual meridional circulation is weakened at middle and high latitudes (Fig. 11, dashed lines) and the polar stratosphere is cooled at polar latitudes (Fig. 10) regardless of whether the tropical heating is applied to equinoctial or wintertime conditions. However, the amplitudes of the differences between the control and perturbed stratospheric residual flow are much more pronounced under equinoctial conditions than under wintertime conditions (Fig. 11).

Figure 12 shows analogous results to those shown in Fig. 10, but for the responses to polar stratospheric cooling. The results in the top panels are reproduced from Fig. 5a; the results in the bottom panels show the responses to the same cooling applied to the wintertime basic state. In the troposphere, the sign of the changes in the extratropical flow and momentum fluxes are again robust to seasonal changes in the basic state (e.g., compare Figs. 12b and 12d). However, the latitude of the tropospheric responses is shifted notably equatorward as the background state is changed from equinoctial to wintertime conditions. The shift in the tropospheric response is in part consistent with the differences between the control climatologies: under equinoctial conditions the jet is centered ~45° latitude (Fig. 1b); under wintertime conditions it is centered ~35° latitude (Fig. 9b).

In the stratosphere, the polar stratospheric cooling drives poleward heat fluxes near 60° latitude and equatorward heat fluxes near 40° latitude regardless of whether the cooling is applied to equinoctial or wintertime conditions (Figs. 12a,c). However, the anomalous poleward heat fluxes are much more pronounced when the cooling is applied to equinoctial conditions. Since the polar stratospheric downgradient heat fluxes are larger under equinoctial conditions (Fig. 12a), it follows that the changes in the polar vortex under equinoctial conditions are damped relative to wintertime conditions (Figs. 12b,d). The smaller differences in poleward heat fluxes between the control and forced runs when the cooling is applied to wintertime conditions (Fig. 12c) suggest that once the polar vortex is established (as in winter), any additional cooling has little further effect on the amount of wave activity that propagates into the polar stratosphere. The weakening of the meridional residual circulation at low latitudes is most pronounced when the polar stratospheric cooling is applied to the wintertime basic state (Fig. 11; gray lines).

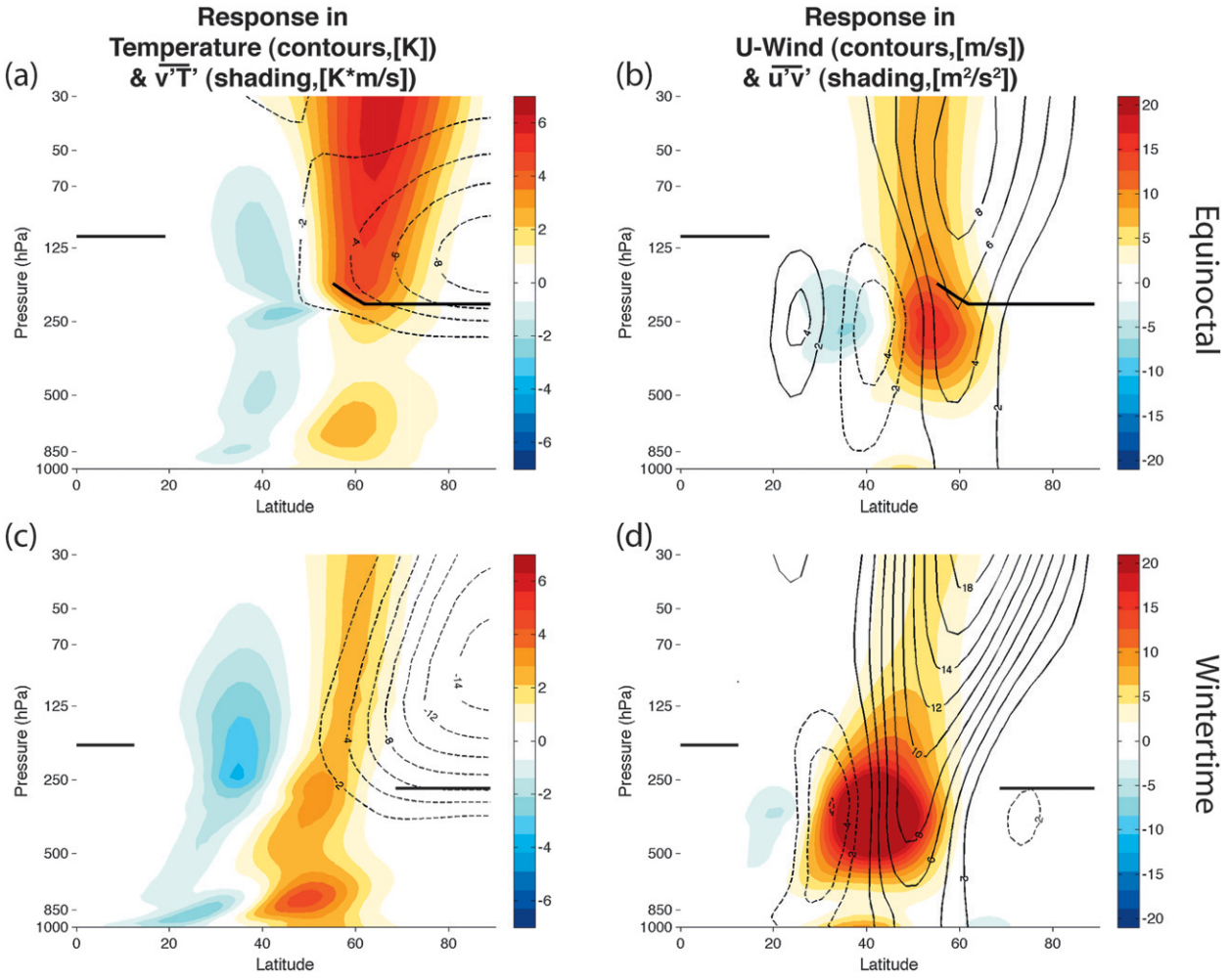

FIG. 12. The zonal-mean response to the polar stratospheric cooling shown in Fig. 5a applied to (top) the equinoctial basic state and (bottom) the wintertime basic state. (left) The total eddy heat flux response (shading) (K m s^{-1}) and the temperature response (contours) (K). (right) The total eddy momentum flux response (shading) (m^2 s^{-2}) and the zonal-mean zonal wind response (contours) (m s^{-1}). Panels (a) and (b) are reproduced from Fig. 5a.

5. Summary and discussion

a. Summary

In this study we examined the structure and robustness of the simple AGCM response to three thermal forcings. The forcings were chosen for their qualitative resemblance to the primary spatially varying heatings associated with anthropogenic climate change: enhanced warming in the tropical troposphere, enhanced cooling in the polar stratosphere, and enhanced warming at the polar surface. We also examined the nonlinearity of the response to multiple forcings and documented the robustness of the principal findings to changes in the basic state.

The results highlight several novel aspects of the AGCM response to thermal forcing.

1) Heating in the tropical troposphere drives a robust poleward contraction of the extratropical storm track and its associated fluxes of heat and momentum (Fig. 2). Similar changes in the storm tracks have been found in fully coupled climate models forced by increasing CO_2 (Fyfe et al. 1999; Kushner et al. 2001; Yin 2005; Miller et al. 2006; Arblaster and Meehl 2006; Lu et al. 2008). At least two studies (Chen and Held 2007; Lu et al. 2008) have argued that the tropical warming found in such simulations plays a key role in the simulated storm-track response, and at least one study has revealed that the latitude of the SH storm track is sensitive to such heating in a full physics AGCM (Lim and Simmonds 2008). The results shown here confirm the robustness of the linkages between tropical heating and the latitude of the storm tracks in the dry dynamical core of an AGCM. The result is robust to seasonal changes in the basic state (Fig. 10), and it suggests that tropical heating

plays a central role in driving the simulated trends in the extratropical storm tracks in IPCC-class climate change simulations (e.g., Miller et al. 2006; Hegerl et al. 2007).

2) Deep cooling in the polar stratosphere also drives a robust poleward contraction of the midlatitude storm track and its associated fluxes of heat and momentum (Fig. 5). The tropospheric circulation response is robust to seasonal changes in the basic state (Fig. 12) and is generally consistent with the response presented in Polvani and Kushner (2002) and Kushner and Polvani (2004). However, when the stratospheric cooling is relatively shallow (~100 hPa), the amplitude and sign of the tropospheric response is strongly dependent on the level of the forcing. In this case, the tropospheric response changes dramatically as the cooling is lifted vertically: when the cooling is centered at 200 hPa, the tropospheric storm track is shifted poleward; when the cooling is centered at 175 hPa, the tropospheric storm track is shifted equatorward; when the cooling is lifted to 150 hPa, the tropospheric response is negligible (Fig. 6). The results suggest that the seemingly robust response of the Southern Hemisphere storm track to Antarctic ozone depletion is dependent not only on the height but also the vertical scale of the associated cooling.
3) Heating in the tropical troposphere is associated with substantial changes in the model stratospheric wave driving. The heating drives anomalously poleward stratospheric heat fluxes near 60° latitude and anomalously equatorward stratospheric heat fluxes near 40° latitude (Figs. 2, 10). Under both equinoctial and wintertime conditions, the changes in the stratospheric heat fluxes are associated with a weakening of the model Brewer–Dobson circulation throughout the extratropics, as indicated by a reduction in the poleward residual flow in the model lower stratosphere (Figs. 4, 11). The changes in the Brewer–Dobson circulation are surprising since they are in the opposite sense of those found in most previous climate change simulations: Rind (1998), Butchart and Scaife (2001), and Li et al. (2008) note a strengthening of the Brewer–Dobson circulation in response to increasing greenhouse gases, and Eichelberger and Hartmann (2005) reveal a strengthening of the Brewer–Dobson circulation in response to prescribed tropical tropospheric heating. However, McLandress and Shepherd (2009) find a weakening of the Brewer–Dobson circulation in SH winter and spring in response to climate change. The weakening of the Brewer–Dobson circulation found here stems from the anomalously equatorward eddy heat fluxes at the tropopause near ~40° latitude (Figs. 2, 10).
4) Deep cooling in the polar stratosphere also drives anomalously poleward stratospheric heat fluxes near 60° latitude and equatorward stratospheric heat fluxes near 40° latitude (Figs. 5, 12). Under equinoctial conditions, the poleward heat fluxes near 60° latitude are substantial, and the stratospheric residual flow is anomalously poleward in the high-latitude stratosphere but anomalously equatorward in the midlatitude stratosphere (Fig. 4). Under wintertime conditions, the poleward heat fluxes near 60° latitude are relatively weak (Fig. 12c), and the equatorward heat fluxes near 40° latitude drive a broader weakening of the model Brewer–Dobson circulation (Fig. 11b). In all cases, the heat fluxes along 60° latitude act to dampen the response of the polar stratospheric temperatures to the imposed diabatic cooling.
5) Warming at the surface over polar regions is associated with an equatorward shift of the tropospheric storm track (Fig. 7). The changes in the model storm track are the same sign as those found during midwinter in coupled climate simulations forced with predicted decreases in Arctic sea ice, albeit the coupled response is only significant during the month of February (Deser et al. 2010). The response of the storm track to surface polar warming is in the opposite sense of the response to tropical tropospheric heating. Though the model lacks realistic planetary waves, which may also play a role in the NH circulation response, the results suggest that the simulated response of the storm track to greenhouse warming is likely to be weaker on average in the NH where polar warming is largest.
6) The model response to the sum of the thermal forcings is structurally similar to but quantitatively very different than the sum of the responses to the individual forcings (Fig. 8). The nonlinearity of the response to multiple forcings complicates predictions of the circulation response to a given thermal forcing, as the response to a single thermal forcing is a function of the other forcings applied to the system.

b. Discussion

What physical processes drive the responses of the model storm track and Brewer–Dobson circulation to thermal forcing? The linear, zonal-mean response to thermal forcing is straightforward and can be deduced from, for example, the balanced vortex equations of Eliassen (1951). The eddy components of the response are more complicated to predict, as they require predicting and quantifying the wave response to changes in the wind and temperature fields. Numerous recent

studies have demonstrated the key role of eddies in the atmospheric response to thermal forcing (e.g., Kushner and Polvani 2004; Son and Lee 2005; Eichelberger and Hartmann 2005; Lorenz and DeWeaver 2007; Simpson et al. 2009), and several studies have offered specific physical hypotheses in an effort to explain the resulting response of the storm tracks (e.g., Lorenz and DeWeaver 2007; Chen and Held 2007; Frierson 2008; Simpson et al. 2009). But as of this writing, the key mechanism(s) that underlie the eddy response to thermal forcing are still open to debate. Below we summarize current hypotheses and discuss their relevance to our results.

1) MECHANISMS RELATED TO THE STORM-TRACK RESPONSE

The mechanisms that may drive the response of the tropospheric storm track can be organized into two broad categories: 1) those associated with vertical gradients in the heating and 2) those associated with meridional gradients in the heating. The former category involves changes in static stability and/or tropopause height. For example, Frierson (2008) argues that increases in tropical and midlatitude tropospheric static stability should act to reduce baroclinic eddy generation on the equatorward side of the storm tracks and thus shift poleward the region of largest eddy generation. Lorenz and DeWeaver (2007) suggest that lifting the tropopause plays a similarly key role in driving the storm track poleward, albeit the causal linkages between the height of the tropopause and the latitude of the storm track remain to be determined.

The latter set of mechanisms involves changes in the meridional temperature gradient at either upper levels or near the surface. Changes in the surface equator-to-pole temperature gradient are thought to play a secondary role in driving the storm track poleward in the IPCC AR4 simulations (Lorenz and DeWeaver 2007). In contrast, changes in the upper-tropospheric temperature gradient are theorized to play a central role, primarily through the associated changes in the upper tropospheric zonal flow. For example, Chen and Held (2007) and Chen et al. (2008) theorize the following series of linkages to explain the causal relationship between tropical warming and/or polar stratospheric cooling and the latitude of the extratropical storm track:

1) Enhanced meridional temperature gradients at upper-tropospheric levels are associated with enhanced westerly flow in the midlatitude upper troposphere/lower stratosphere via the thermal wind relation;
2) the phase speed of Rossby waves is directly related to the amplitude of the background flow, and hence the enhanced westerly flow in the upper midlatitude troposphere leads to increased phase speeds there;
3) a component of the eddies in the midlatitude troposphere propagate equatorward and "break" where the background flow matches the eddy phase speed, so that waves with anomalously high phase speeds break at anomalously poleward latitudes in the subtropics;
4) the associated changes in the convergence of the eddy momentum flux in the subtropics drive a thermally damped meridional circulation cell that enhances the tropospheric baroclinicity in middle latitudes; and
5) the enhanced lower-tropospheric baroclinicity draws the region of largest wave generation and hence heat fluxes poleward, ultimately shifting the location of the storm tracks poleward (see also Robinson 2000).

How relevant are the above mechanisms for the storm-track responses revealed here? As suggested in Lorenz and DeWeaver (2007), the effects of changes in surface baroclinicity appear to be secondary, in that the same amplitude forcing yields a much larger eddy response when applied at upper levels rather than at the surface (e.g., compare Figs. 2 and 7). The linkages between tropopause height and the storm tracks proposed in Lorenz and DeWeaver (2007) also hold for all of the runs in this study but for one notable exception: the lifting of the polar stratospheric cooling in Fig. 6 induces an equatorward shift in the model storm track, whereas Lorenz and DeWeaver's mechanism predicts a poleward shift due to the raising of the tropopause. We view the height of the tropopause as indicative of the induced changes in the atmospheric circulation but not necessarily a forcing mechanism in its own right. Likewise, the mechanism proposed by Frierson (2008) is consistent with the responses to the tropical tropospheric heating shown here, but it does not provide an explanation for the changes in the tropospheric response as the polar stratospheric cooling is lifted.

The mechanism provided by Chen and Held (2007) and Chen et al. (2008) and outlined above seemingly provides a physically consistent explanation for all of the results shown in this study. The tropical heating and polar stratospheric cooling are both associated with westerly wind anomalies in the upper troposphere/lower stratosphere and thus their mechanism holds—at least qualitatively—for the response to both these thermal forcings. The mechanism also appears to provide a qualitative explanation for the change in the tropospheric response as the polar cooling is lifted with height. For example, the instantaneous response to the shallow polar cooling should be associated with out-of-phase potential

vorticity anomalies above and below the cooling region, with cyclonic vorticity anomalies immediately above the cooling but anticyclonic vorticity anomalies immediately below the cooling. We hypothesize that, if the region of largest climatological eddy momentum fluxes in the upper troposphere/lower stratosphere is overlain by westerly anomalies in the instantaneous (linear) response, then the phase speeds of the majority of eddies will become anomalously westerly and the storm track will be shifted poleward. However, if the region of largest climatological eddy momentum fluxes in the upper troposphere/lower stratosphere is overlain by easterly anomalies, then the phase speeds of the majority of eddies will become anomalously easterly and the storm track will be shifted equatorward.

2) Mechanisms that may drive the Brewer–Dobson response

The simulated changes in the stratospheric Brewer–Dobson circulation can be interpreted in the context of poleward shifts in the vertical propagation of wave activity in the lowermost stratosphere. At 100 hPa, the responses to both tropical warming and polar stratospheric cooling are associated with a reduction in vertical wave propagation (i.e., anomalously equatorward heat fluxes) near 40° latitude but an increase in vertical wave propagation near 60° latitude. In the case of the tropical warming, the former reduction is larger than the latter increase, and the residual meridional circulation is anomalously equatorward. In the case of polar stratospheric cooling, the amplitude of the heat fluxes along 60° latitude varies considerably from equinoctial to wintertime conditions, and thus so does the response of the model Brewer–Dobson circulation: under equinoctial conditions, the anomalous poleward heat fluxes near 60° latitude are large and the residual meridional circulation is anomalously poleward at high latitudes but equatorward at midlatitudes; under wintertime conditions, the anomalous poleward heat fluxes near 60° latitude are small and the residual meridional circulation is anomalously equatorward at nearly all latitudes.

As is the case for the mechanisms that drive the response of the tropospheric storm track, the mechanisms that drive the response of the wave-driven Brewer–Dobson circulation can be divided into two general themes: 1) changes in the source of eddy activity at tropospheric levels (e.g., Butchart and Scaife 2001; Rind et al. 2002; Eichelberger and Hartmann 2005) and 2) changes in the configuration of the lower-stratospheric background flow (e.g., Garcia and Randel 2008; Sigmond and Scinocca 2010). Both mechanisms seem to be important in our experiments. On the one hand, the vertical coherence of the changes in the heat fluxes from the surface to the middle stratosphere in, for example, Fig. 2, suggests that the anomalous wave fluxes at stratospheric levels are driven in part by the anomalous wave fluxes in the troposphere. On the other hand, the differences in the eddy heat flux response to the same polar stratospheric cooling applied to wintertime and equinoctial conditions (Fig. 12) indicate that the configuration of the stratospheric flow also plays a key role in determining the model Brewer–Dobson circulation response. In this case, strengthening the vortex beyond its wintertime state seems to have little effect on the amount of wave activity that propagates into the polar stratosphere.

The physical mechanisms that determine the signs and amplitudes of both the tropospheric and stratospheric eddy responses will be investigated quantitatively in a companion paper (Butler and Thompson 2010, unpublished manuscript).

Acknowledgments. We thank David Randall for use of the CSU AGCM and computing hours at the National Energy Research Scientific Computing Center (NERSC). We also thank Dargan Frierson, Gang Chen, Mike Wallace, Susan Solomon, and Paul Kushner for helpful comments on the research, and three anonymous reviewers for constructive and insightful comments on the manuscript. Amy Butler was funded in part by the United States Environmental Protection Agency (EPA) under the Science to Achieve Results (STAR) Graduate Fellowship Program. David W. J. Thompson was funded by the NSF Climate Dynamics Program. This work was partially funded by the U.S. DOE under Cooperative Agreement DE-FC02-06ER64302 to Colorado State University.

REFERENCES

Andrews, D. G., J. R. Holton, and C. B. Leovy, 1987: *Middle Atmosphere Dynamics*. Academic Press, 489 pp.

Arblaster, J., and G. Meehl, 2006: Contributions of external forcings to southern annular mode trends. *J. Climate,* **19,** 2896–2905.

Brandefelt, J., and E. Kallen, 2004: The response of the Southern Hemisphere atmospheric circulation to an enhanced greenhouse gas forcing. *J. Climate,* **17,** 4425–4442.

Bretherton, C., M. Widmann, V. Dymnikov, J. Wallace, and I. Blade, 1999: The effective number of spatial degrees of freedom of a time-varying field. *J. Climate,* **12,** 1990–2009.

Butchart, N., and A. Scaife, 2001: Removal of chlorofluorocarbons by increased mass exchange between the stratosphere and troposphere in a changing climate. *Nature,* **410,** 799–802.

Cai, W., P. Whetton, and D. Karoly, 2003: The response of the Antarctic Oscillation to increasing and stabilized atmospheric CO_2. *J. Climate,* **16,** 1525–1538.

Chan, C. J., and R. A. Plumb, 2009: The response to stratospheric forcing and its dependence on the state of the troposphere. *J. Atmos. Sci.,* **66,** 2107–2115.

Chen, G., and I. Held, 2007: Phase speed spectra and the recent poleward shift of Southern Hemisphere surface westerlies. *Geophys. Res. Lett.,* **34,** L21805, doi:10.1029/2007GL031200.

——, J. Lu, and D. M. W. Frierson, 2008: Phase speed spectra and the latitude of surface westerlies: Interannual variability and global warming trend. *J. Climate,* **21,** 5942–5959.

Deser, C., R. Tomas, M. Alexander, and D. Lawrence, 2010: The seasonal atmospheric response to projected Arctic sea ice loss in the late twenty-first century. *J. Climate,* **32,** 333–351.

Eichelberger, S. J., and D. L. Hartmann, 2005: Changes in the strength of the Brewer-Dobson circulation in a simple AGCM. *Geophys. Res. Lett.,* **32,** L15807, doi:10.1029/2005GL022924.

Eliassen, A., 1951: Slow thermally or frictionally controlled meridional circulation in a circular vortex. *Astrophys. Norv.,* **5,** 19–20.

Frierson, D., 2008: Midlatitude static stability in simple and comprehensive general circulation models. *J. Atmos. Sci.,* **65,** 1049–1062.

——, J. Lu, and G. Chen, 2007: Width of the Hadley cell in simple and comprehensive general circulation models. *Geophys. Res. Lett.,* **34,** L18804, doi:10.1029/2007GL031115.

Fu, Q., C. M. Johanson, J. M. Wallace, and T. Reichler, 2006: Enhanced mid-latitude tropospheric warming in satellite measurements. *Science,* **312,** 1179.

Fyfe, J., G. Boer, and G. Flato, 1999: The Arctic and Antarctic oscillations and their projected changes under global warming. *Geophys. Res. Lett.,* **26,** 1601–1604.

Garcia, R., and W. J. Randel, 2008: Acceleration of the Brewer–Dobson circulation due to increases in greenhouse gases. *J. Atmos. Sci.,* **65,** 2731–2739.

Gerber, E., and G. Vallis, 2007: Eddy–zonal flow interactions and the persistence of the zonal index. *J. Atmos. Sci.,* **64,** 3296–3311.

——, and L. Polvani, 2009: Stratosphere–troposphere coupling in a relatively simple AGCM: The importance of stratospheric variability. *J. Climate,* **22,** 1920–1933.

——, S. Voronin, and L. Polvani, 2008: Testing the annular mode autocorrelation time scale in simple atmospheric general circulation models. *Mon. Wea. Rev.,* **136,** 1523–1536.

Gillett, N., and D. W. J. Thompson, 2003: Simulation of recent Southern Hemisphere climate change. *Science,* **302,** 273–275.

Haigh, J., M. Blackburn, and R. Day, 2005: The response of tropospheric circulation to perturbations in lower-stratospheric temperature. *J. Climate,* **18,** 3672–3685.

Hegerl, G. C., and Coauthors, 2007: Understanding and attributing climate change. *Climate Change 2007: The Physical Science Basis,* S. Solomon et al., Eds., Cambridge University Press, 663–745.

Heikes, R. P., and D. A. Randall, 1995: Numerical integration of the shallow water equations on a twisted icosahedral grid. Part I: Basic design and results of tests. *Mon. Wea. Rev.,* **123,** 1862–1880.

Held, I. M., and M. J. Suarez, 1994: A proposal for the intercomparison of the dynamical cores of atmospheric general circulation models. *Bull. Amer. Meteor. Soc.,* **75,** 1825–1830.

Hurrell, J. W., 1995: Decadal trends in the North Atlantic Oscillation region temperatures and precipitation. *Science,* **269,** 676–679.

Konor, C., and A. Arakawa, 1997: Design of an atmospheric model based on a generalized vertical coordinate. *Mon. Wea. Rev.,* **125,** 1649–1673.

Kushner, P., and L. Polvani, 2004: Stratosphere–troposphere coupling in a relatively simple AGCM: The role of eddies. *J. Climate,* **17,** 629–639.

——, I. Held, and T. Delworth, 2001: Southern Hemisphere atmospheric circulation response to global warming. *J. Climate,* **14,** 2238–2249.

Li, F., J. Austin, and J. Wilson, 2008: The strength of the Brewer–Dobson circulation in a changing climate: Coupled chemistry–climate model simulations. *J. Climate,* **21,** 40–57.

Lim, E.-P., and I. Simmonds, 2008: Effect of tropospheric temperature change on the zonal mean circulation and SH winter extratropical cyclones. *Climate Dyn.,* **33,** 19–32, doi:10.1007/s00382-008-0444-0.

Lorenz, D. J., and E. T. DeWeaver, 2007: Tropopause height and zonal wind response to global warming in the IPCC scenario integrations. *J. Geophys. Res.,* **112,** D10119, doi:10.1029/2006JD008087.

Lu, J., G. A. Vecchi, and T. Reichler, 2007: Expansion of the Hadley cell under global warming. *Geophys. Res. Lett.,* **34,** L06805, doi:10.1029/2006GL028443.

——, G. Chen, and D. Frierson, 2008: Response of the zonal mean atmospheric circulation to El Niño versus global warming. *J. Climate,* **21,** 5835–5851.

McLandress, C., and T. G. Shepherd, 2009: Simulated anthropogenic changes in the Brewer–Dobson circulation, including its extension to high latitudes. *J. Climate,* **22,** 1516–1540.

Miller, R. L., G. A. Schmidt, and D. T. Shindell, 2006: Forced annular variations in the 20th century Intergovernmental Panel on Climate Change Fourth Assessment Report models. *J. Geophys. Res.,* **111,** D18101, doi:10.1029/2005JD006323.

Norton, W. A., 2003: Sensitivity of the Northern Hemisphere surface climate to simulation of the stratospheric polar vortex. *Geophys. Res. Lett.,* **30,** 1627, doi:10.1029/2003GL016958.

Overland, J. E., and M. Wang, 2005: The Arctic climate paradox: The recent decrease of the Arctic Oscillation. *Geophys. Res. Lett.,* **32,** L06701, doi:10.1029/2004GL021752.

Polvani, L. M., and P. J. Kushner, 2002: Tropospheric response to stratospheric perturbations in a relatively simple general circulation model. *Geophys. Res. Lett.,* **29,** 1114, doi:10.1029/2001GL014284.

Rind, D., 1998: Latitudinal temperature gradients and climate change. *J. Geophys. Res.,* **103,** 5943–5971.

——, P. Lonergan, N. K. Lonergan, and D. Shindell, 2002: 2 x CO_2 and solar variability influences on the troposphere through wave-mean flow interactions. *J. Meteor. Soc. Japan,* **80,** 863–876.

Ring, M. J., and R. A. Plumb, 2007: Forced annular mode patterns in a simple atmospheric general circulation model. *J. Atmos. Sci.,* **64,** 3611–3626.

——, and ——, 2008: The response of a simplified GCM to axisymmetric forcings: Applicability of the fluctuation–dissipation theorem. *J. Atmos. Sci.,* **65,** 3880–3898.

Ringler, T. D., R. P. Heikes, and D. A. Randall, 2000: Modeling the atmospheric general circulation using a spherical geodesic grid: A new class of dynamical cores. *Mon. Wea. Rev.,* **128,** 2471–2490.

Robinson, W. A., 1991: The dynamics of the zonal index in a simple model of the atmosphere. *Tellus,* **43A,** 295–305.

——, 2000: A baroclinic mechanism for the eddy feedback on the zonal index. *J. Atmos. Sci.,* **57,** 415–422.

Seidel, D. J., and W. J. Randel, 2007: Recent widening of the tropical belt: Evidence from tropopause observations. *J. Geophys. Res.,* **112,** D20113, doi:10.1029/2007JD008861.

——, Q. Fu, W. J. Randel, and T. J. Reichler, 2008: Widening of the tropical belt in a changing climate. *Nat. Geosci.,* **1,** 21–24.

Shindell, D. T., and G. A. Schmidt, 2004: Southern Hemisphere climate response to ozone changes and greenhouse gas increases. *Geophys. Res. Lett.,* **31,** L18209, doi:10.1029/2004GL020724.

——, R. Miller, G. Schmidt, and L. Pandolfo, 1999: Simulation of recent northern winter climate trends by greenhouse-gas forcing. *Nature,* **399,** 452–455.

Sigmond, M., and J. F. Scinocca, 2010: The influence of the basic state on the Northern Hemisphere circulation response to climate change. *J. Climate,* **23,** 1434–1446.

Simpson, I. R., M. Blackburn, and J. D. Haigh, 2009: The role of eddies in driving the tropospheric response to stratospheric heating perturbations. *J. Atmos. Sci.,* **66,** 1347–1365.

Son, S., and S. Lee, 2005: The response of westerly jets to thermal driving in a primitive equation model. *J. Atmos. Sci.,* **62,** 3741–3757.

——, and Coauthors, 2008: The impact of stratospheric ozone recovery on the Southern Hemisphere westerly jet. *Science,* **320,** 1486–1489.

Thompson, D., and S. Solomon, 2002: Interpretation of recent Southern Hemisphere climate change. *Science,* **296,** 895–899.

——, J. Wallace, and G. Hegerl, 2000: Annular modes in the extratropical circulation. Part II: Trends. *J. Climate,* **13,** 1018–1036.

Yin, J. H., 2005: A consistent poleward shift of the storm tracks in simulations of 21st century climate. *Geophys. Res. Lett.,* **32,** L18701, doi:10.1029/2005GL023684.

Yu, J., and D. Hartmann, 1993: Zonal flow vacillation and eddy forcing in a simple GCM of the atmosphere. *J. Atmos. Sci.,* **50,** 3244–3259.